Atmospheric
Chemistry
and Physics
Discussions

Open Access

PM$_{2.5}$ pollution in a megacity of southwest China: source apportionment and implication

J. Tao[1], J. Gao[2], L. Zhang[3], R. Zhang[4], H. Che[5], Z. Zhang[1], Z. Lin[1], J. Jing[6], J. Cao[7], and S.-C. Hsu[8]

[1]South China Institute of Environmental Sciences, Ministry of Environmental Protection, Guangzhou, China
[2]Chinese Research Academy of Environmental Sciences, Beijing, China
[3]Air Quality Research Division, Science Technology Branch, Environment Canada, Toronto, Canada
[4]RCE-TEA, Institute of Atmospheric Physics, Chinese Academy of Sciences, Beijing, China
[5]Key Laboratory of Atmospheric Chemistry (LAC), Institute of Atmospheric Composition, Chinese Academy of Meteorological Sciences (CAMS), China
[6]Centre for Atmosphere Watch and Services (CAWAS), Meteorological Observation Center of CMA, Beijing, China
[7]Key Laboratory of Aerosol, SKLLQG, Institute of Earth Environment, Chinese Academy of Sciences, Xi'an, China
[8]Research Center for Environmental Changes (RCEC), Academia Sinica, Taipei, Taiwan

ACPD

14, 5147–5196, 2014

Source apportionment of PM$_{2.5}$ in a megacity of southwest China

J. Tao et al.

Title Page

Abstract	Introduction
Conclusions	References
Tables	Figures

|◀ | ▶|

◀ | ▶

Back | Close

Full Screen / Esc

Printer-friendly Version

Interactive Discussion

Source apportionment of PM$_{2.5}$ in a megacity of southwest China

J. Tao et al.

Discussion Paper | Discussion Paper | Discussion Paper | Discussion Paper | Discussion Paper

Abstract

Daily PM$_{2.5}$ (aerosol particles with an aerodynamic diameter of less than 2.5 µm) samples were collected at an urban site in Chengdu, an inland megacity in southwest China, during four one-month periods in 2011, with each period in a different season.

5 Samples were subjected to chemical analysis for various chemical components ranging from major water-soluble ions, organic carbon (OC), element carbon (EC), trace elements to biomass burning tracers, anhydrosugar levoglucosan (LG) and mannosan (MN). Two models, ISORROPIA-II thermodynamic equilibrium model and positive matrix factorization (PMF) model, were applied to explore the likely chemical forms of ionic

10 constituents and to apportion sources for PM$_{2.5}$. Distinctive seasonal patterns of PM$_{2.5}$ and associated main chemical components were identified and could be explained by varying emission sources and meteorological conditions. PM$_{2.5}$ showed a typical seasonality of waxing in winter and waning in summer, with an annual mean of 119 µg m^{-3}. Mineral soil concentrations increased in spring whereas biomass burning species ele-

15 vated in autumn and winter.

Six major source factors were identified to have contributed to PM$_{2.5}$ using the PMF model. These were secondary inorganic aerosols, coal combustion, biomass burning, iron and steel manufacturing, Mo-related industries, and soil dust, and they contributed 37 ± 18 %, 20 ± 12 %, 11 ± 10 %, 11 ± 9 %, 11 ± 9 %, and 10 ± 12 %, respectively,

20 to PM$_{2.5}$ masses on annual average, while exhibiting large seasonal variability. On annual average, the unknown emission sources that were not identified by the PMF model contributed 1 ± 11 % to the measured PM$_{2.5}$ mass. Various chemical tracers were used for validating PMF performance. Antimony (Sb) was suggested to be a suitable tracer of coal combustion in Chengdu. Results of LG and MN helped constrain

25 the biomass burning sources, with wood burning dominating in winter and agricultural waste burning dominating in autumn. Excessive Fe (Ex-Fe), defined as excessive portion in measured Fe that cannot be sustained by mineral dust, is corroborated to be a straightforward useful tracer of iron and steel manufacturing pollution. In Chengdu,

Mo/Ni mass ratios were persistently higher than unity, and considerably distinct from those usually observed in ambient airs. V/Ni ratios averaged at only 0.7. Results revealed that heavy oil fuel combustion should not be a vital anthropogenic source, and additional anthropogenic sources for Mo are yet to be identified. Overall, the emission sources identified in Chengdu could be dominated by local sources located in the vicinity of Sichuan, a result differed from those found in Beijing and Shanghai, wherein cross-boundary transport is significant in contributing pronounced $PM_{2.5}$. These results provided implications for $PM_{2.5}$ control strategies.

1 Introduction

Fine particulate matter ($PM_{2.5}$) – those having an aerodynamic diameter of less than 2.5 µm, is a key air pollutant in terms of adverse human health effects and visibility degradation (Pope III and Dockery, 2006; Watson, 2002). The specialized cancer agency of the World Health Organization (WHO), the International Agency for Research on Cancer (IARC), has classified outdoor PM as carcinogenic to humans (Group 1) (http://www.iarc.fr/). For instance, daily mortality has been found to be related to the level of $PM_{2.5}$ sourced from traffic emission and coal combustion in six US cities (Laden et al., 2000). $PM_{2.5}$ is a complex mixture of sulfate, nitrate, ammonium, water, organic and element carbon, soil dust, trace elements, and persistent organic pollutants. It originates from both natural and anthropogenic sources, and includes both primary and secondary particle species. Knowledge of sources and their contributions to $PM_{2.5}$ is crucial in making feasible policies for controlling $PM_{2.5}$ level to protect human health and reduce hazy weather occurrence.

Source apportionment of $PM_{2.5}$ has been achieved extensively around the world (Lee and Kang, 2001; Putaud et al., 2004; Hueglin et al., 2005; Lonati et al., 2005; Chen et al., 2010). Such technique has been increasingly applied for the past decade in China, although mostly focused on urban cities and areas such as Beijing, Yangtze River Delta (YRD), and Pearl River Delta (PRD) (He et al., 2001; Ye et al., 2003; Tao

et al., 2012; Zhang et al., 2013). To date, PM$_{2.5}$ pollution is still a severe problem in China. Sichuan Basin is one of the most polluted regions in China (Cao et al., 2007; Zhao et al., 2010; Yang et al., 2011), as demonstrated by the spatial distribution of aerosol optical depth (AOD) retrieved by satellites (Fig. 1).

Chengdu, located west of Sichuan Basin (Fig. 1), is one of the megacities in China with a population of more than 10 million. This megacity is one of the few inland megacities worldwide which are far from oceans. Air pollution is a serious issue for this city, presumably due to the complex topography surrounding the city and huge amounts of coal consumption. For example, PM$_{2.5}$ concentrations reached an annual mean of 165 μg m^{-3} in 2009 to 2010, which is five times higher compared with the new national ambient air quality standards (NAAQS) (35 μg m^{-3}) and 16 times higher compared with the air quality guideline (10 μg m^{-3}) recommended by the WHO (Tao et al., 2013). Achieving NAAQS in this city is apparently a challenging task. A better understanding of PM$_{2.5}$ sources and their relative contributions is urgently needed to enact effective emission control policies and to implement multi-pollutant reduction measures. To date, studies on seasonal-based source apportionments remain lacking, yet they are critical in shedding lights on emission control measures of air pollutants and in making emission control policies (Tao et al., 2013). To fill these gaps, a comprehensive data set acquired in 2011 is analyzed in the present study, with an emphasis on seasonal-based source apportionments.

Accordingly, the present study aims to accomplish the following goals: to systematically characterize PM$_{2.5}$ levels and their chemical compositions on seasonal and annual basis, to identify PM$_{2.5}$ source factors and to quantify their respective contributions, and to evaluate existing and recommend new environmental protection measures based on novel source apportionment results.

2 Methodology

2.1 Site description

PM$_{2.5}$ samples were collected at the Chengdu Research Academy of Environmental Sciences (CRAES) located in the urban area of Chengdu (30.65° N, 104.03° E) (Fig. 1). Instruments used in this study were installed on the roof (21 m above ground) of an office building of the CRAES. This site was built with unimpeded vision, although a residential area and a park were situated about 100 m east from the sampling site. In 2004, the Chengdu municipal government promulgated the "Chengdu Plan of Industrial Development Layout (2003–2020)", which forbids any pollution industries within the third-ring road inside the city (http://www.cdgy.gov.cn/Article/2004/200402/1165.html). The CRAES site is within and more than 5 km away from the third-ring road (Fig. S1). Therefore, no major stationary air pollution sources were present within a circumference of 5 km of the site, except mobile emissions; but the site was affected by industrial pollutions outside the third-ring road. Thus, the site was considered to be representative of a typical urban environment in Chengdu.

2.2 Sampling

PM$_{2.5}$ samples were collected using two low-flow air samplers (MiniVol TAC, AirMetrics Corp., Eugene, OR, USA). Prior to the start of the sampling campaign, the flow rate of PM$_{2.5}$ samplers was calibrated. Samples were collected at a flow rate of 5 L min^{-1} on two types of filters: 47 mm quartz fiber filter (Whatman QM-A) and 47 mm Teflon filter (Whatman PTFE). Quartz filters were pre-baked at 800 °C for 3 h prior to sampling. Collected filters were stored in a freezer at −18 °C before chemical analysis to minimize evaporation of volatile components.

A total of 117 PM$_{2.5}$ samples and 12 blank samples were collected in 2011 during the following periods: 6–30 January (representative of winter), 3 April–3 May (spring), 1–31 July (summer), and 1–31 October (autumn). Collection duration of each sample

was 24 h, starting at 10:00 LT each day and ending at 10:00 the following day. Three field blanks were collected with each sampler during every seasonal campaign, which were then analyzed together with the samples.

2.3 Gravimetric weighing

Teflon filters were measured gravimetrically for particle mass concentration using a Sartorius MC5 electronic microbalance with a sensitivity of ±1 µg (Sartorius, Göttingen, Germany) after 24 h equilibration at $23 \pm 1\,^\circ\mathrm{C}$ with relative humidity at $40 \pm 5\,\%$. Each filter was weighed at least three times before and after sampling. Differences among replicate weights were mostly less than 20 µg for each sample. Net mass was obtained by subtracting pre-weight from post-weight.

2.4 Chemical analysis

2.4.1 OC and EC

An area of $0.526\,\mathrm{cm}^2$ punch from each quartz filter was analyzed for eight carbon fractions following the IMPROVE_ A thermal/optical reflectance (TOR) protocol on a DRI model 2001 carbon analyzer (Atmoslytic, Inc., Calabasas, CA, USA) (Chow et al., 2007). This analysis acquired four OC fractions (OC1, OC2, OC3, and OC4 at 140, 280, 480, and 580 $^\circ$C, respectively, in a helium [He] atmosphere), OP (a pyrolyzed carbon fraction determined when transmitted laser light attains its original intensity after oxygen [O_2] was added to the analysis atmosphere), and three EC fractions (EC1, EC2, and EC3 at 580, 740, and 840 $^\circ$C, respectively, in a 2 % O_2/98 % He atmosphere). IMPROVE_ TOR OC is operationally defined as OC1 + OC2 + OC3 + OC4 + OP and EC is defined as EC1 + EC2 + EC3 − OP (Chow et al., 2007).

2.4.2 Trace elements and water-soluble ions

Each PTFE filter was cut into two equal halves with ceramic scissors, and then subjected to extraction and digestion. One half was extracted with ultrapure water for ionic measurement and the other half was dissolved with acids for elemental measurement. Digestion was performed with an acid mixture ($5\,mL\,HNO_3 + 2\,mL\,HF$) by using an ultra-high throughput microwave digestion system (MARSXpress, CEM, Matthews, NC). A blank reagent and two filter blanks were prepared in each run following the same procedures adopted for the samples. All acids used in this study were of ultra-pure grade (Merck, Germany). The detailed digestion method has been published elsewhere (Hsu et al., 2008, 2010). A suite of trace elements in the digestion solutions, including Al, Fe, Na, Mg, K, Ca, Sr, Ba, Ti, Mn, Co, Ni, Cu, Zn, Mo, Ag, Cd, Sn, Sb, Tl, Pb, V, Cr, As, Y, Se, Zr, Nb, Ge, Rb, Cs, Ga, U and 15 rare earth elements (REEs), were analyzed by inductively coupled plasma–mass spectrometry (ICP-MS). Quality assurance and control of ICP-MS measurement was guaranteed by the analysis of a certified reference standard, NIST SRM-1648 (urban particulates). Resulting recoveries fell within ±10 % of the certified values for most elements, except for Se, As, Cs, Sb, and Rb (±15 %) (Zhang et al., 2013).

Silicon was quantified using X-ray fluorescence analysis (XRF, Epsilon5, PANalytical Company, the Netherlands) on Teflon filters before acid digestion. Quality assurance/quality control (QA/QC) procedures of the XRF analysis have been described in Xu et al. (2012a).

The other half of all filter samples was used for extraction with 20 mL ultrapure water (specific resistivity = 18.2 MΩ cm; Millipore, Massachusetts, United States) for 1 h. Analysis of extract solutions was performed with an ion chromatograph (Dionex ICS-900 and ICS-1100) equipped with a conductivity detector (ASRS-ULTRA). A Dionex AS11-HC separator column was used for analyzing F^-, Cl^-, NO_3^-, and SO_4^{2-}. A CS12A separator column was used to analyze Na^+, NH_4^+, K^+, Mg^{2+}, and Ca^{2+}. The eluents used were 22 mM to 25 mM KOH for anions and 20 mM methansulfonic acid (MSA) for

cations. In general, method detection limits (MDL) were within the range of $0.01\,\mu g\,m^{-3}$ to $0.04\,\mu g\,m^{-3}$ for cations and $0.03\,\mu g\,m^{-3}$ to $0.07\,\mu g\,m^{-3}$ for anions (Hsu et al., 2007).

2.4.3 Sugar measurements

A $2.0\,cm^2$ punch from each quartz filter was extracted in $2\,mL$ of ultrapure water under ultrasonic agitation for 1 h. Extracts were filtered through a syringe filter (pore size $0.25\,\mu m$, PTFE, Whatman, USA) to remove insoluble materials. Anhydrosugar levoglucosan (LG) and mannosan (MN) were measured by a Dionex ICS-3000 system. Instrumental controls, data acquisition, and chromatographic integration were performed using Dionex Chromeleon software. A calibration was performed for each analytical sequence. The DL for LG and MN were $0.002\,mg\,L^{-1}$. A detailed description of the analytical method can be found elsewhere (Tao et al., 2013; Engling et al., 2006; Iinuma et al., 2009).

2.5 Measurements of meteorological parameters

Meteorological parameters including wind direction, wind speed, relative humidity (RH), temperature, and precipitation were measured every 10 min. Wind direction and wind speed were recorded by a wind monitor (Vaisala Company, Helsinki, Finland, Model QMW101). Ambient RH and temperature were measured by an RH/temperature probe (Vaisala Company, Helsinki, Finland, Model QMH101). Precipitation was measured using a rain gauge (Vaisala Company, Helsinki, Finland, Model QMR101). Both meteorological instruments were mounted at 3 m above the roof of the CRAES building (24 m above ground). Solar radiation data were obtained from a national meteorological station ($30.7°$ N, $103.8°$ E) located 20 km from CRAES.

2.6 Data analysis methods

To analyze chemical mass closure of $PM_{2.5}$, $PM_{2.5}$ mass was reconstructed as the sum of organic matter (OM), EC, inorganic ions, water content, fine soil (FS), and trace element oxides (TEO). The factor converting OC to OM was 1.6 for spring and summer, and 1.8 for autumn and winter, as explained in Sect. 3.1.2. Water content was calculated using the thermodynamic equilibrium model-ISORROPIA II (reserve mode) (Fountoukis and Nenes, 2007). To evaluate the model performance, statistical metrics including mean bias (MB), normalized mean bias (NMB), normalized mean error (NME) and the root mean-square error (RMSE) were calculated as below (Eder and Yu, 2006):

$$MB = \frac{1}{N} \sum_{1}^{N} (C_m - C_o) \tag{1}$$

$$NMB = \frac{\sum_{1}^{N} (C_m - C_o)}{\sum_{1}^{N} C_o} 100\% \tag{2}$$

$$NME = \frac{\sum_{1}^{N} |C_m - C_o|}{\sum_{1}^{N} C_o} 100\% \tag{3}$$

$$RMSE = \sqrt{\frac{1}{N} \sum_{1}^{N} (C_m - C_o)^2} \tag{4}$$

where C_m and C_o are modeled and observed concentration of total inorganic ions, respectively.

The FS component was estimated using the following formula (Malm et al., 1994):

$$[FS] = 2.20[Al] + 2.49[Si] + 1.63[Ca] + 2.42[Fe] + 1.94[Ti] \tag{5}$$

However, Si is mostly volatilized as SiF_4 in acid digestion when using HF. Thus, we used Si data analyzed by XRF, whereas the data for other four elements were obtained from ICP-MS measurement.

For TEO, the contribution of heavy metals as metal oxides was estimated using the following equation (Zhang et al., 2013):

$$TEO = 1.3 \times [0.5 \times (Sr + Ba + Mn + Co + Rb + Ni + V)$$
$$+ 1.0 \times (Cu + Zn + Mo + Cd + Sn + Sb + Tl + Pb + As + Se + Ge + Cs + Ga)] \quad (6)$$

Source apportionment analysis was conducted using positive matrix factorization (PMF) Model Version 3.0 of EPA, US (Norris et al., 2008). To reduce uncertainties of PMF results, chemical components with annual average concentrations below MDLs were removed, such as F^- and REEs, which are essentially similar to the major crustal elements such as Al. Thirty-five chemical components were used for the PMF model, including OC, EC, LG, Na^+, NH_4^+, K^+, Mg^{2+}, Ca^{2+}, Cl^-, NO_3^-, SO_4^{2-}, Al, Fe, Mg, Ca, Sr, Ba, Ti, Mn, Ni, Cu, Zn, Mo, Cd, Sn, Sb, Tl, Pb, V, Cr, As, Se, Zr, Ge, Rb, Cs and Ga.

Three-day backward trajectories were calculated at two elevations of 500 and 1500 m for every sampling day starting at 02:00 UTC (10:00 LT) using the HYSPLIT 4 trajectory model (http://ready.arl.noaa.gov/HYSPLIT.php) to investigate synoptic patterns and transport routes of air masses. The model adopted meteorological data from FNL (final operational global analysis) as input.

3 Results and discussion

3.1 General characteristics of PM$_{2.5}$ and chemical components

3.1.1 PM$_{2.5}$ mass

The annual average of PM$_{2.5}$ mass concentrations in Chengdu was $119 \pm 56 \, \mu g \, m^{-3}$ (Table 1), which was three times higher than the NAAQS for annual PM$_{2.5}$ ($35 \, \mu g \, m^{-3}$). As summarized in Table 1, PM$_{2.5}$ level in Chengdu was only significantly lower than one inland megacity, Xi'an ($194 \, \mu g \, m^{-3}$), located in northwest China (Zhang et al., 2011), and was comparable with the other two megacities, Chongqing ($129 \, \mu g \, m^{-3}$) (Yang

et al., 2011), also located in Sichuan Basin, and Beijing (135 $\mu g m^{-3}$) (Zhang et al., 2013). However, $PM_{2.5}$ in Chengdu was much higher than those observed in coastal megacities, such as Tianjin (90 $\mu g m^{-3}$) (Gu et al., 2010), Shenyang (75 $\mu g m^{-3}$) (Ma et al., 2011), Shanghai (90 $\mu g m^{-3}$) (Feng et al., 2009), Fuzhou (44 $\mu g m^{-3}$) (Xu et al., 2012b), Xiamen (86 $\mu g m^{-3}$) (Zhang et al., 2012), Guangzhou (76 $\mu g m^{-3}$) (Tao et al., 2014) and Hong Kong (57 $\mu g m^{-3}$) (Louie et al., 2005). The annual average $PM_{2.5}$ in Chengdu was even higher by a factor of 3 to 15 compared with those in other developed countries (Balasubramanian et al., 2003; Heo et al., 2009; Khan et al., 2009; Pinto et al., 2004; Querol et al., 2004). Thus, Chengdu suffered from severe $PM_{2.5}$ pollution problem and experienced the highest $PM_{2.5}$ level worldwide.

A typical seasonal variation in $PM_{2.5}$ mass concentrations was observed (Table 2), with higher concentrations in winter (158 $\mu g m^{-3}$) and spring (126 $\mu g m^{-3}$) and lower concentrations in autumn (111 $\mu g m^{-3}$) and summer (89 $\mu g m^{-3}$). Generally, $PM_{2.5}$ levels are governed by emissions, transportation, chemical transformation, and depositional processes, which are all related to meteorological conditions. However, systematic investigations on $PM_{2.5}$ emission inventories have not been conducted in Sichuan (including Chengdu). The highest wintertime $PM_{2.5}$ concentration could be partly related to certain weather conditions in terms of low mixing height because of weak solar radiation (Fig. S2). By contrast, the lowest summertime concentration was in part, due to frequent rainfall (Fig. S1), which led to efficient removal of suspended particles from the atmosphere (Wang et al., 2010).

3.1.2 Carbonaceous aerosols and biomass burning markers

Annual mean concentrations of OC and EC were 17 ± 8 and $7 \pm 4 \mu g m^{-3}$, accounting for $PM_{2.5}$ masses of $14.3 \pm 4.4 \%$ and $5.7 \pm 1.5 \%$, respectively (Table 2). Seasonal variation of EC was similar to that of $PM_{2.5}$, following the order of winter ($8 \pm 8 \mu g m^{-3}$) > spring ($7 \pm 5 \mu g\, m^{-3}$) ≥ autumn ($7 \pm 3 \mu g m^{-3}$) > summer ($6 \pm 3 \mu g m^{-3}$). However, the seasonal pattern of OC was somewhat different from that of EC and $PM_{2.5}$, with the

second highest season in autumn ($20 \pm 9\,\mu g\,m^{-3}$) instead of in spring ($15 \pm 7\,\mu g\,m^{-3}$). The distinct seasonality between OC and EC implies likely changes in the strength of their respective sources in different seasons. LG concentrations were nearly identical in autumn ($659 \pm 441\,ng\,m^{-3}$) and winter ($635 \pm 246\,ng\,m^{-3}$), followed by spring ($235 \pm 151\,ng\,m^{-3}$) and summer ($152 \pm 89\,ng\,m^{-3}$), with an annual mean of $412 \pm 352\,ng\,m^{-3}$. However, MN showed a more typical seasonality compared with LG, with a maximum ($80 \pm 34\,ng\,m^{-3}$) in winter, followed by autumn ($36 \pm 27\,ng\,m^{-3}$), spring ($19 \pm 17\,ng\,m^{-3}$), and summer ($9 \pm 7\,ng\,m^{-3}$). The levels of these two markers were much higher than those measured in European countries, such as Sweden (Szidat et al., 2009), Belgium (Zdráhal et al., 2001), Switzerland (Szidat et al., 2006) and Norway (Yttri et al., 2009).

Sources of carbonaceous aerosols can be further qualitatively evaluated by the relationship of OC against EC (Turpin and Huntzicker, 1995) and biomass burning markers against OC or EC (Szidat et al., 2009). For instance, large discrepancies and variability in OC/EC ratios reportedly exist in coal combustion (0.3–7.6), vehicle emission (0.7–2.4), and biomass burning (4.1–14.5) (Watson et al., 2001). As shown in Fig. 2a, OC and EC in Chengdu were well correlated in each season, with R^2 ranging from 0.65 to 0.85. Mean OC/EC ratios increased from 2.0 in spring and 1.8 in summer to 2.9 in autumn and 2.6 in winter. These average ratios were lower than those (3.3) measured in PM_{10} in Chengdu in 2006, but within the range found across China by Zhang et al. (2008a). Good correlations between OC and EC, but distinct OC/EC ratios suggest that OC and EC were derived from similar sources that varied seasonally. As depicted in Fig. 2b and c, LG correlated with OC and MN, with the LG/OC ratio ranging from 0.015 in summer to 0.034 in winter and the LG/MN ratios ranging from 7.8 in winter to 17 in autumn. In addition to the differences in seasonal ratios, correlations were also quite variable from season to season with the highest coefficient ($R^2 \geq 0.90$) in winter and the lowest ($R^2 < 0.60$) in summer. Again, features of biomass burning biomarker revealed that biomass burning sources of carbonaceous aerosols varied with the season. LG/OC ratio has been applied as a tracer of wood burning (Szidat et al., 2009, and references therein), whereas LG/MN ratio has been used for

distinguishing specific types of biomass burning (Engling et al., 2009). High LG/OC ratio (0.029) and low LG/MN ratio (7.8) in winter may indicate dominance of wood burning (Szidat et al., 2009; Oliveira et al., 2007; Pio et al., 2008). By contrast, high LG/OC (0.034) and LG/MN (17) ratios in autumn could reveal combined sources of
5 wood burning together with rice straw and other agricultural waste burning (Sheesley et al., 2003; Engling et al., 2009). These suggestions are in agreement with the fact that residents in Chengdu used to utilize waste wood as energy source to generate heat in cold winter. In addition to residential use, waste wood was used by nearly one thousand smaller coal boilers (less than 10 ton vapor h^{-1}). Agricultural waste burning
10 was usually most severe in harvest season – autumn, in China (Duan et al., 2004). Our LG/OC ratios were much lower than those (~ 0.135) typically detected in wood burning (Szidat et al., 2009, and references therein) as OC was produced from additional sources besides biomass burning. Using this characteristic ratio (none was available in China), we estimated an annual contribution of 3.1 µg m^{-3} (varying from 1.1 µg m^{-3}
15 to 4.9 µg m^{-3} in the four seasons) from wood burning, which represents 18 % of the observed total OC (ranging from 11 % to 24 % in varying seasons) in Chengdu. The annual mean proportion is lower than that (~ 30 %) acquired from PMF modeling, which is presented below. This finding indicates that biomass burning other than wood burning sources (e.g., agricultural waste burning) accounted for the rest of the contributions
20 (i.e., ~ 10 %) to the OC.

Lei et al. (2011) reported that the 2005 primary OC and EC emissions from anthropogenic sources in China were 1.51 and 3.19 Tg, respectively. In Sichuan province, the residential sector was the largest contributor, constituting 47 % to black carbon (BC) and 81 % to OC. In other regions of China, the dominant sector could be differ-
25 ent. For example, the industrial sector is dominant in northern China provinces, such as Hebei, Shanxi, Shandong and Henan. According to Qin and Xie (2012), annual BC emission from Sichuan in 2009 has increased to over 0.14 Tg. Coal was still the most predominant fuel used in China, which alone contributed nearly 50 % to the national BC emission (Qin and Xie, 2012). Based on the coincidence of OC/EC ratios between

the PM$_{2.5}$ aerosols (annual mean ~ 2.4) and emissions (~ 2.1), coal combustion appeared to be an important source of carbonaceous aerosols throughout the year. The factor converting OC to OM has been suggested to vary with its dominant sources and the age of organic aerosols (Turpin and Lim, 2001; Andreae et al., 2008). In the present study, a value of 1.6 was adopted for spring and summer, and 1.8 for autumn and winter. These values were consistent with those recently observed across China (Xing et al., 2013), although slightly lower than those found across the US, which had a median value of 1.80 to 1.95 (Simon et al., 2011).

3.1.3 Water-soluble ions

Water-soluble ions also comprised important constituents of PM$_{2.5}$. The sum of all the major water-soluble ions averaged at $52 \pm 29 \, \mu g \, m^{-3}$ in Chengdu (Table 2), accounting for $42 \pm 9 \%$ of PM$_{2.5}$ mass. SO_4^{2-}, NO_3^-, and NH_4^+ were the dominant ions, and their combination constituted $90 \pm 5 \%$ of total ion concentrations. To investigate the associations among ions, a thermodynamic equilibrium model, ISORROPIA II (Fountoukis and Nenes, 2007), was applied to simulate chemical components and phase state of major ions in thermodynamic equilibrium conditions. Water and inorganic salt concentrations were simultaneously estimated by ISORROPIA II model (reserve mode) at a fixed relative humidity (RH 40 %) and temperature (23 °C). Seven compounds that had concentrations larger than zero were derived (Table 3). On annual average, the total concentrations of all inorganic chemical species calculated by ISORROPIA II model was $51 \pm 28 \, \mu g \, m^{-3}$, which was very close to the sum of all the observed ions concentrations ($52 \pm 29 \, \mu g \, m^{-3}$). To evaluate ISORROPIA II model performances, the statistical parameters MB, NMB, NME and RMSE for total ion concentrations were calculated by Eqs. (1)–(4).The MB, NMB, NME and RMSE values are −1.2, −2.3 %, 2.3 % and 1.6, suggesting that the ISORROPIA II model can reasonably simulate most of the observed ions. Both SO_4^{2-} and NO_3^- were mostly associated with NH_4^+, present in the forms of $(NH_4)_2SO_4$ and NH_4NO_3. All Cl$^-$ were exclusively present in the form

of NH_4Cl. Besides NH_4^+, the other four cations (K^+, Na^+, Ca^{2+}, and Mg^{2+}) were also associated with SO_4^{2-}. Seasonal variations in concentrations of the predominant chemical species, $(NH_4)_2SO_4$ and NH_4NO_3, were consistent with those of SO_4^{2-} and NO_3^- concentrations that showed the highest concentrations in winter and the lowest in summer or autumn (Table 2). Liquid water derived by the ISORROPIA II model reached to $15.0 \pm 8.4\ \mu g\,m^{-3}$ on the average, following similar seasonal patterns of major ions.

3.1.4 Metal elements

Daily concentrations of FS and TEO were calculated using Eqs. (5) and (6). Annual concentrations of FS and TEO were 6.7 ± 4.4 and $1.1 \pm 0.6\ \mu g\,m^{-3}$, which accounted for $6.3 \pm 4.8\,\%$ and 0.9 ± 0.3 %, respectively, of $PM_{2.5}$ mass. Seasonal concentrations of FS decreased from $10.1\ \mu g\,m^{-3}$ in spring to $5.5\ \mu g\,m^{-3}$ in autumn and $5.4\ \mu g\,m^{-3}$ in winter and summer. For TEO, seasonal variability was relatively small, declining from $1.3\ \mu g\,m^{-3}$ in spring to $1.1\ \mu g\,m^{-3}$ in winter, $1.0\ \mu g\,m^{-3}$ in autumn, and $0.9\ \mu g\,m^{-3}$ in summer. Both FS and TEO concentrations similarly waxed in spring, with small fluctuations seen in the other seasons.

The total concentration of all the trace metals (i.e., excluding Al, Fe, Na, Mg, K and Ca) was $0.8 \pm 0.4\ \mu g\,m^{-3}$, constituting 0.7 ± 0.3 % of $PM_{2.5}$ mass. As, Cd, Co, Cr, Ni, Pb and Se are well-known carcinogenic heavy metals registered in the US Agency for Toxic Substances and Disease Registry. Noticeably, the annual mean concentration of As in Chengdu exceeded the WHO standard ($6.6\ ng\,m^{-3}$, lifetime risk level is $1:100\,000$) by a factor of 3. Twenty-five of the 117 samples exceeded $5\ ng\,m^{-3}$ Cd concentration, which is the WHO's guide value.

Enrichment factors (EFs) relative to the earth's upper crust composition can be used for assessing the anomaly of elemental composition of aerosol particles. In this study, Al served as a reference element. Average composition of earth crust was referred to Hans Wedepohl (1995). The EFs of Zr, Ca, Mg, Ti, Sr, Fe, Ba, V, Na and K were less than 10; EFs of Rb, Mn, Ni, Cs, Cr, Ga and Ge ranged from 10 to 100; and EFs of Cu,

Tl, Mo, Sn, Zn, Pb, As, Sb, Cd and Se were larger than 100 (Fig. 3). The EFs of carcinogenic heavy metals, As, Cd, Co, Cr, Ni, Pb and Se, were 1772 ± 1091, 6060 ± 3942, 6 ± 5, 47 ± 31, 25 ± 21, 1753 ± 814, and 6095 ± 3261, respectively, indicating that these heavy metals were of anthropogenic origins, except for Co, which was further analyzed below by the PMF results. Therefore, carcinogenic heavy metal pollution, especially As, in Chengdu was serious. Control strategies must be undertaken to alleviate heavy metal loadings.

3.2 Reconstructed PM$_{2.5}$ mass

The PM$_{2.5}$ mass in Chengdu was reconstructed on seasonal and annual basis by employing the methods described in Sect. 2.6. PM$_{2.5}$ mass concentrations could be reconstructed by combining the main components, as depicted in Fig. 4. The correlations (R^2) between the reconstructed and measured mass concentrations were higher than 0.93 in all the seasons and the seasonal average mass ratio ranged from 0.90 to 0.99. On average, the reconstructed masses explained $92 \pm 11\%$ of measured ones, indicating a good performance of the formulations applied. Based on the results, PM$_{2.5}$ in the urban area of Chengdu composed of OM, EC, FS, TEO, inorganic ions, and water, with contributions of $24.5 \pm 8.4\%$, $5.7 \pm 1.5\%$, 6.3 ± 4.8 %, $0.9 \pm 0.3\%$, $42.2 \pm 9.0\%$, and $12.2 \pm 3.0\%$, respectively.

As illustrated in Fig. 5, the total of inorganic ions was the largest contributor to PM$_{2.5}$, accounting for a relatively constant fraction of 40 % to 44 % in the four seasons. Contributions of EC, TEO, and water to PM$_{2.5}$ were relatively constant from season to season. However, seasonal variations were evident for the contributions of OM and FS to PM$_{2.5}$, with OM contributed 19.4 %, 19.8 %, 33.4 % and 25.6 % in spring, summer, autumn and winter, respectively, and FS contributed 9.3 %, 6.4 %, 5.3 % and 3.7 %, respectively. These results suggest that biomass burning and soil dust had contrasting trends in contributing to PM$_{2.5}$, with more OM contributions in autumn and winter and more dust contributions in spring and summer.

3.3 Source apportionment

Based on the PMF modeling results, six main source factors were identified, including secondary inorganic aerosols, coal combustion, biomass burning, iron and steel industry, Mo-related industry and soil dust. Modeled source profiles together with the rela-
5 tive contributions of individual sources to each analyzed species are shown in Fig. 6. Their contributions are summarized in Table 4. The annual and seasonal averages of the absolute ($\mu g\,m^{-3}$) and fractional (%) contributions from each source were calculated based on their daily values simulated by PMF model. As expected, the annual averages of absolute and fractional contributions from identified sources, except the
10 obvious seasonal sources – biomass burning and soil dust, are larger than their respective standard deviations. This suggests that the PMF results might be reasonable. To further confirm this assumption, the modeled time-series of the contributions from each source was compared with the observed time-series of certain chemical species that could represent respective sources (Fig. 7).
15   The first source comprises secondary inorganic aerosols, characterized by high NH_4^+, SO_4^{2-}, and NO_3^- concentrations (Fig. 6a) (Zhang et al., 2013). The PMF-derived secondary inorganic aerosols accounted for $37 \pm 18\%$ of the $PM_{2.5}$ (Table 4). These secondary products were formed from the oxidation of main precursor gases, SO_2 and NO_x, that were mainly emitted from coal combustion, vehicle exhausts, and even
20 biomass burning, which in turn interacted with NH_3 emitted mainly from agricultural activities and livestock waste. Ammonium ion is a typical secondary pollutant that is often a good tracer of secondary inorganic aerosols. As expected, temporal variations of secondary inorganic aerosol and NH_4^+ concentrations were coincident (Fig. 7a), with R^2 of 0.76.
25   The second source is coal combustion, characterized by high EC, Zn, Cu, Sn, Sb, Tl and Pb concentrations (Fig. 6b). This source represented a mean contribution of $20 \pm 12\%$ to $PM_{2.5}$, with a maximal absolute contribution ($\sim 29\,\mu g\,m^{-3}$) in spring and winter (Table 4), which agrees with the seasonal distribution of coal consumption in

Title Page

Abstract | Introduction

Conclusions | References

Tables | Figures

|◄ | ►|

◄ | ►

Back | Close

Full Screen / Esc

Printer-friendly Version

Interactive Discussion

China. Coal combustion was the most dominant contributor of national CO_2 emission in China, representing 72 % (Gregg et al., 2008). In Sichuan, the main sources were industrial coal boilers and residential coal stoves, the latter had significantly higher emissions of EC (Zhang et al., 2008b). Residential coal stoves were forbidden in Chengdu and thus smaller industrial coal boilers dominated this factor. Leaded gasoline has been phased out since 2000 in China and coal combustion became the primary source of Pb aerosols in China. This source accounted for 31 % of the observed Pb in Chengdu (Fig. 6b) (Mukai et al., 2001). Dan et al. (2004) attributed the observed high Pb and Zn in wintertime $PM_{2.5}$ in Beijing to the coal combustion source. From a global perspective, coal combustion is the primary contributor of global emissions of Sb, Sn, and Tl in the atmosphere (Pacyna and Pacyna, 2001). According to a recent estimate, atmospheric Sb emission from China was up to 818 metric tons per year, of which 61.8 % was emitted from coal combustion and the remaining 26.7 % was from nonferrous metal smelting (Tian et al., 2012). However, Sb was sometimes attributable to traffic emissions, particularly in urban areas (Sternbeck et al., 2002). For Sichuan, the quota of coal combustion in atmospheric Sb emission can reach 85 %. Based on our PMF results, coal combustion contributed 48 % of the observed Sb in Chengdu. As a consequence, PMF-derived time series of coal combustion contribution and our observed Sb are in good covariation (Fig. 7b). This result further implies that Sb, at least in Sichuan Basin, could be an effective tracer of coal combustion primary pollutants.

The third source factor is biomass burning, characterized by elevated OC, EC, LG, K^+, NO_3^-, and Cl^- (Fig. 6c). This result can be corroborated by the results of Tao et al. (2013), which showed that significant amounts of OC, EC, LG, Cl^- and K^+ existed in local biomass burning smoke at a suburban site of Chengdu. LG has been demonstrated as a good tracer of biomass burning (Engling et al., 2009, and references therein). This factor accounted for 11 ± 10 % of the $PM_{2.5}$ mass concentration. Contributions from this source factor to $PM_{2.5}$ were higher in autumn (19 ± 11 %) and winter (16 ± 7 %) than in spring (7 ± 6 %) and summer (1 ± 5 %) (Table 4), consistent with seasonal patterns of LG concentration. As expected, variation trends of biomass

Source apportionment of $PM_{2.5}$ in a megacity of southwest China

J. Tao et al.

Title Page

Abstract	Introduction
Conclusions	References
Tables	Figures

◀◀ ▶▶

◀ ▶

Back | Close

Full Screen / Esc

Printer-friendly Version

Interactive Discussion

burning and LG mass concentrations were similar (Fig. 7) and a good correlation between them was found ($R^2 = 0.77$). Noticeably, the LG concentration ($235\,\mathrm{ng\,m^{-3}}$) observed in this study, i.e., spring 2011, was around 40 % lower than that ($397\,\mathrm{ng\,m^{-3}}$) in spring 2009. This result is ascribed to the fact that Chengdu municipal government established a special management committee to control biomass burning in suburban areas.

The fourth source factor is the iron and steel industry, characterized by high Fe, Mn, Zn, Pb, Cu, Cr, As and Ga concentrations (Fig. 6d). This factor contributed 11 ± 9 % to the $PM_{2.5}$ mass concentration (Table 4). From single-particle analyses, enrichment of Fe, Zn, and Pb was observed in ambient atmospheric particles around a major integrated steelwork in UK (Dall'Osto et al., 2008). China ranks as the largest iron and steel producer worldwide, whose productions constitute 44.2 % of the global production in 2010 (http://www.miit.gov.cn/n11293472/n11293832/n11293907/n11368223/14344076.html). However, only a few source apportionment studies separately identified this source in terms of its contributions to $PM_{2.5}$ pollution and PM-bound chemicals in China (Querol et al., 2006; Ni et al., 2012), despite that it was well recognized as a main source of pollutants, such as polycyclic aromatic hydrocarbons (PAHs) (Yang et al., 2002) and heavy metals (Machemer, 2004). Fe, Mn and Cr in ambient aerosols collected around industrial sites were categorized into steel-related metals (Sweet et al., 1993). In the present study, we found a considerably practicable tracer – Ex-Fe, for this important emission source that seems to have been overlooked in China thus far. As illustrated in Fig. 8a, scatter plots of Fe vs. Al in $PM_{2.5}$ of Chengdu show that most samples had Fe/Al mass ratios higher than 0.60, a characteristic ratio of Asian dust (Hsu et al., 2013, and references therein). During our sampling period, a dust storm sample was collected on 30 April 2011, which gave rise to an Al maximum ($3408\,\mathrm{ng\,m^{-3}}$). This sample had a Fe/Al ratio of 0.63 (Fig. 8a), in agreement with the typical ratio. The correlation result is also consistent with the EF_{crust} result showing that the annual mean EF_{crust} of Fe is 3.6 (Fig. 3), which is significantly higher than unity. This finding demonstrates that fine Fe aerosols originated from other non-natural (i.e.,

Source apportionment of $PM_{2.5}$ in a megacity of southwest China

J. Tao et al.

Title Page

Abstract | Introduction

Conclusions | References

Tables | Figures

|◀ | ▶|

◀ | ▶

Back | Close

Full Screen / Esc

Printer-friendly Version

Interactive Discussion

anthropogenic) sources aside from dust. Likewise, the Mn/Al ratios ranged from 0.073 to 0.145 in the four seasons (Fig. 8b), which are significantly larger than that (0.015) in average crust (Taylor, 1964). This result is indicative of enrichment and thus, the dominance of other sources aside from natural dust. Accordingly, we defined Ex-Fe and excessive Mn (Ex-Mn) as follows:

$$[\text{Ex-Fe}] = [\text{Fe}_{\text{Measured}}] - [\text{Al}_{\text{Measured}}] \times 0.60$$
$$[\text{Ex-Mn}] = [\text{Mn}_{\text{Measured}}] - [\text{Al}_{\text{Measured}}] \times 0.015$$

where $\text{Al}_{\text{Measured}}$, $\text{Fe}_{\text{Measured}}$, and $\text{Mn}_{\text{Measured}}$ denote the measured concentrations of Al, Fe, and Mn, respectively, and the factors of 0.60 and 0.015 are the Fe/Al and Mn/Al mass ratios, respectively, in average crust composition. We then compared the derived time-series of Ex-Fe and the iron and steel source contribution and found that they have a strong correlation ($R^2 = 0.72$). Furthermore, we explored the correlations of steel-related metals, such as Mn, Ex-Mn, Zn and Cr, against the derived Ex-Fe (Machemer, 2004), as depicted in Fig. S3. Obvious linear correlations were observed, with R^2 ranging from 0.28 to 0.81, demonstrating that the iron and steel industry could be a vital source, in agreement with the PMF results (Fig. 6d).

Notably, the iron and steel manufacturing sources contributed more As than coal combustion sources in Chengdu (i.e., 48 % vs. 19 %) (Fig. 6d). As is considered one of the more useful tracers of coal combustion, along with Se (Hsu et al., 2009). The As/Se ratio in $PM_{2.5}$ in Chengdu averaged 6.8 ± 2.6, which is much higher than that in coal combustion emission in Sichuan (1.1) and across China (0.94) (Tian et al., 2010). This finding suggests that coal combustion is not the main contributor of fine aerosol As and merits further investigation in other provinces/cities, thus facilitates emission estimation of this carcinogenic metal, namely, As across China. Moreover, contributions from this source to $PM_{2.5}$ varied significantly with season, ranging from 19 ± 9 % in summer to 11 ± 8 % in autumn, 8 ± 7 % in spring and 5 ± 4 % in winter. Seasonality may be relevant to variability in production capacities of iron smelting factories. In fact, air pollutants (SO_2,

Full Screen / Esc

Printer-friendly Version

Interactive Discussion

NO$_2$, and PM$_{10}$) emitted from certain most productive manufacturers around Chengdu were higher in summer than in other seasons based on routine monitoring results.

The fifth source is the Mo-related industry, characterized by high Mo and Ni. This source contributed 11±9 % to the PM$_{2.5}$ mass concentration but varied seasonally, e.g., 14 ± 7 % in autumn, 13 ± 5 % in winter, 11 ± 14 % in summer, and 8 ± 5 % in spring (Table 4). Six samples had Mo concentrations over 10 ng m^{-3}, of these three occurred in autumn and the other three in winter. The EF$_{crust}$ values of Mo and Ni in fine aerosols in Chengdu were ∼ 500 and ∼ 30 (Fig. 3), respectively, which are much higher than unity, indicative of the dominance of anthropogenic origins. Atmospheric Mo can originate from traffic emission, biomass burning, and industrial activities (Tsukuda et al., 2005; Dongarrá et al., 2007; Alleman et al., 2010). It usually has a concentration lower than 1 ng m^{-3} (Negral et al., 2008; Alleman et al., 2010; Mooiborek et al., 2011); in contrast, measurements in this study showed a mean concentration of 3.8 ± 3.8 ng m^{-3}. Sn, Sb, and Cr were not found in the source profiles of this factor (Fig. 6e), suggesting that traffic emissions should not be a significant source for these elements, although Sb is often enriched in aerosols from vehicle emissions (Gómez et al., 2005; Varrica et al., 2013). Much higher OC/EC ratio (∼ 100) also rules out the likelihood of traffic emission. This factor can be discriminated from the second and fourth factors, i.e., coal combustion and iron and steel industry, as the missing three metals are representatives of the latter two source factors, as discussed above. For Ni, heavy oil combustion has often been suggested to be its most important anthropogenic source along with non-ferrous smelters (Sweet et al., 1993). Heavy oil combustion in Chengdu appeared to be an insignificant source for Ni, as V/Ni ratio was averaged at only 0.7 ± 0.3, which is much lower than the value (2–4) characterized for this industry sector (Almeida et al., 2005; Mamane et al., 2008). Furthermore, Mo and Ni correlated with each other in every season (Fig. 9), despite their ratio (Mo/Ni) varied with season with higher ratios (1.7–1.9) in autumn and winter and lower ratios (1.0–1.3) in spring and summer. This trait is a distinctive feature (Mo-rich and Ni-deplete) from what is usually found in ambient atmosphere, e.g., a ratio significantly lower than unity (Negral et al., 2008; Mooibroek

et al., 2011; Alleman et al., 2010). This factor may indicate the existence of a specific Mo source with a characteristic Mo/Ni ratio of 2.0 or higher, as demonstrated by the dashed line in Fig. 9. It is thus designated as the Mo-related industry, which warrants further investigations, particularly in terms of which specific industry it belongs to. This finding is comparable with the result in Pittsburgh, where source apportionment studies have found Mo and Cr association with a source factor called specialty steel factor (Pekney et al., 2006). The time-series of this source contribution and the observed Mo concentrations correlated very well with R^2 of 0.47.

The sixth source factor is soil dust, which is characterized by elevated Al, Fe, Mg, Ca, Sr, Ti, V and Zr. This factor accounted for $10 \pm 10\%$ of the $PM_{2.5}$ mass concentration, which is much lower than that (15 %) in Beijing (Zhang et al., 2013). The contribution of soil dust to $PM_{2.5}$ mass concentrations was much higher in spring ($18 \pm 17\%$) than in other seasons ($9 \pm 12\%$, $8 \pm 7\%$ and $4 \pm 5\%$. in summer, autumn, and winter, respectively). This seasonal pattern is also consistent with that of the FS concentration. The soil dust factor covers desert dust that usually prevails in spring and comes from north China via long-range transport, fugitive dust, and street dust, among which the latter two were dominated by local sources. Al, Fe, Ca and Ti are typically major crustal elements that are often used to calculate soil dust mass concentration (Malm et al., 1994), similar to what was done in the current study. The EFs of Al, Fe, Mg, Ca, Sr, Ti, V, and Zr were lower than 10, indicative of the dominance of a natural mineral origin. Aluminum is a good tracer of soil dust. As expected, the time series of soil dust contribution and Al concentrations were consistent (Fig. 7f), with R^2 of 0.85.

3.4 Implications for PM alleviation

Efforts have been exerted to improve air quality in Chengdu in the past five years, as summarized in Table 5. The Chengdu municipal government decreed that all industrial factories must be relocated out of Chengdu urban area by the end of 2007. Commercial and residential coal combustion was forbidden in urban areas. A special management committee was established for controlling biomass burning in suburban areas. New

light motor vehicles have been evaluated using the Chinese state emission standard IV since 2011. Heavy motor vehicles were forbidden in central urban areas and were evaluated using Chinese state emission standard III in 2013. Hybrid electric vehicles have been widely used in public transportation system in recent years. These control strategies have not effectively alleviated the $PM_{2.5}$ pollution. Annual mean concentration of $PM_{2.5}$ in Chengdu was still nearly three times higher than NAAQS ($35\,\mu g\,m^{-3}$), implying that tremendous efforts are still needed.

Our study offers new insights into the causes of the elevated $PM_{2.5}$ levels. Despite the fact that all industrial enterprises in Chengdu urban areas had been relocated, most of these were resettled in Qingbaijiang industrial zone and Jintang county, which are situated at the upwind region around 20 km north of Chengdu. According to the spatial distribution of the fine AOD retrieved from moderate resolution imaging spectroradiometer sensors onboard Terra and Aqua satellites (Fig. 1), the highest AOD (> 0.6) distributed in Sichuan Basin centered at the two biggest cities (Chengdu and Chongqing). Effective measures are also needed over the entire basin. Air mass back trajectories calculated using the NOAA HYSPLIT 4 trajectory model (Fig. 10) showed that air masses arrived at CRAES station at 500 and 1500 m levels, but originated from the northeastern and western directions, often passed over Deyang, Mianyang, and Meishan Cities, where many industrial emission facilities are located. The combination of source apportionment results in conjunction with satellite AOD image and trajectory analyses suggest the dominance of local anthropogenic sources instead of regional and/or natural sources.

According to the PMF results, fossil fuel combustion-related activities including source factors of secondary inorganic aerosols, coal combustion, iron and steel manufacturing, and Mo-related industry, contributed nearly 80 % to $PM_{2.5}$ and 96 % to sulfate aerosols. Therefore, coal quality in terms of sulfur and heavy metal content, and coal usage in Sichuan Province should be managed, whereas PM concentration in coal combustion-generated emissions should be abated. It is noted that traffic emission was not identified as a major factor by the PMF although the number of motor

vehicles in Chengdu has exceeded two million. This raised the postulation that the management of traffic pollution might be effective to certain extent and that the traffic emission is relatively insignificant in contributing to the $PM_{2.5}$ pollution. It should be noted that emissions from the traffic might be incorporated into the source factor of soil dust as its weighting contents of Zn, Pb, Cu, Sn, and Sb were relatively elevated, and into the factor of secondary inorganic aerosols. Thus, more studies are needed to explore the contributions of traffic emissions to $PM_{2.5}$ pollution. In addition, biomass burning activities are presently a tough issue for China's environmental protection administration. Biomass fuel is widely used for cooking in rural areas in China. Waste straws produced in harvest seasons are habitually burned for fertilizing soils. The law forbidding straw burning was only enacted recently. A common strategy used by small boiler industries in Sichuan is to replace coal with biomass fuel as an energy source considering that sulfur dioxide emissions from biomass fuels may be much lower than from coal (Andreae and Merlet, 2001). However, more effort is needed in reducing air pollutant emissions from small boilers, which requires establishing new air pollutant emission standards for biomass fuel boilers. Rigorous efforts should be jointly exerted by different regions and cities and at various levels of the government.

4 Conclusions

The annual average $PM_{2.5}$ concentration reached $119 \pm 56\,\mu g\,m^{-3}$ in 2011 in Chengdu, an inland megacity of southwest China. A typical seasonality of waxing in winter and waning in summer was observed. The annual $PM_{2.5}$ level in this city was three times greater than the NAAQS standard ($35\,\mu g\,m^{-3}$) and higher than those in many cities around the world. Annual mean concentration of carcinogenic As in Chengdu was up to $20 \pm 11\,ng\,m^{-3}$, which is also three times higher than the WHO's guide value ($6.6\,ng\,m^{-3}$). Based on the results of chemical measurements and ISORROPIA-II thermodynamic equilibrium model results, major components of fine aerosols were identified to be inorganic ions, organic matter, elemental carbon, mineral soils, trace

element oxides, and water, the sum of which accounted for $92 \pm 11\%$ of the observed masses.

Six source factors were identified using the PMF source apportionment model. The absolute ($\mu g\,m^{-3}$) and fractional (%) contributions from each source factor varied with season. Distinctive chemical species were successfully used as characteristic tracers of individually modeled sources to validate source apportionment results. Biomarkers of biomass burning, LG and MN, were applied to constrain the more likely biomass burning sources. Wood burning was identified to be the main source in winter while agricultural waste burning was in autumn. The present study found a straightforward surrogate of iron and steel manufacturing pollution, namely, excessive Fe, which is well correlated to the contribution from this source. A special source, Mo-related heavy industries, was modeled by PMF, corresponding to a persistently high Mo/Ni ratio of ≥ 1.0 throughout the sampling period. A preliminarily hypothesis could be that the special source was relevant to specific alloy industries and/or military industries, pending further investigations.

The high $PM_{2.5}$ levels in Chengdu were mainly dominated by local anthropogenic emissions in the territory of Sichuan Basin, in contrast to those found in Beijing. Unique topography surrounding the city is conducive to air pollutant accumulation and enhance $PM_{2.5}$ pollution. Stricter emissions standards are needed to alleviate elevated $PM_{2.5}$ loadings in this region. The source apportionment results presented here could serve as a valuable scientific base in enacting effective emission control measures and policies.

Supplementary material related to this article is available online at http://www.atmos-chem-phys-discuss.net/14/5147/2014/ acpd-14-5147-2014-supplement.pdf.

References

Alleman, L. Y., Lamaison, L., Perdrix, E., Robache, A., and Galloo, J.-C.: PM_{10} metal concentrations and source identification using positive matrix factorization and wind sectoring in a French industrial zone, Atmos. Res., 96, 612–625, doi:10.1016/j.atmosres.2010.02.008, 2010.

Almeida, S., Pio, C., Freitas, M., Reis, M., and Trancoso, M.: Source apportionment of fine and coarse particulate matter in a sub-urban area at the Western European Coast, Atmos. Environ., 39, 3127–3138, doi:10.1016/j.atmosenv.2005.01.048, 2005.

Andreae, M. O. and Merlet, P.: Emission of trace gases and aerosols from biomass burning, Global Biogeochem. Cy., 15, 955–966, doi:10.1029/2000GB001382, 2001.

Balasubramanian, R., Qian, W., Decesari, B. S., Facchini, M. C., and Fuzzi, S.: Comprehensive characterization of $PM_{2.5}$ aerosols in Singapore, J. Geophys. Res., 108, 4523, doi:10.1029/2002JD002517, 2003.

Cao, J., Lee, S., Chow, J. C., Watson, J. G., Ho, K., Zhang, R., Jin, Z., Shen, Z., Chen, G., and Kang, Y.: Spatial and seasonal distributions of carbonaceous aerosols over China, J. Geophys. Res.-Atmos., 112, D22S11, doi:10.1029/2006JD008205, 2007.

Chen, L.-W. A., Lowenthal, D. H., Watson, J. G., Koracin, D., Kumar, N., Knipping, E. M., Wheeler, N., Craig, K., and Reid, S.: Toward effective source apportionment using positive matrix factorization: experiments with simulated $PM_{2.5}$ data, J. Air Waste Manage. Assoc., 60, 43–54, doi:10.3155/1047-3289.60.1.43, 2010.

Chow, J. C., Watson, J. G., Chen, L.-W. A., Chang, M. O., Robinson, N. F., Trimble, D., and Kohl, S.: The IMPROVE_ a temperature protocol for thermal/optical carbon analysis: maintaining consistency with a long-term database, J. Air Waste Manage. Assoc., 57, 1014–1023, doi:10.3155/1047-3289.57.9.1014, 2007.

Dall'Osto, M., Booth, M., Smith, W., Fisher, R., and Harrison, R. M.: A study of the size distributions and the chemical characterization of airborne particles in the vicinity of a large integrated steelworks, Aerosol Sci. Tech., 42, 981–991, doi:10.1080/02786820802339587, 2008.

Dongarrà, G., Manno, E., Varrica, D., and Vultaggio, M.: Mass levels, crustal component and trace elements in PM_{10} in Palermo, Italy, Atmos. Environ., 41, 7977–7986, doi:10.1016/j.atmosenv.2007.09.015, 2007.

Title Page

Abstract | Introduction

Conclusions | References

Tables | Figures

|◄ | ►|

◄ | ►

Back | Close

Full Screen / Esc

Printer-friendly Version

Interactive Discussion

Duan, F., Liu, X., Yu, T., and Cachier, H.: Identification and estimate of biomass burning contribution to the urban aerosol organic carbon concentrations in Beijing, Atmos. Environ., 38, 1275–1282, doi:10.1016/j.atmosenv.2003.11.037, 2004.

Eder, B. and Yu, S.: A performance evaluation of the 2004 release of Models-3 CMAQ, Atmos. Environ., 40, 4811–4824, doi:10.1016/j.atmosenv.2005.08.045, 2006.

Engling, G., Carrico, C. M., Kreidenweis, S. M., Collett Jr, J. L., Day, D. E., Malm, W. C., Lincoln, E., Min Hao, W., Iinuma, Y., and Herrmann, H.: Determination of levoglucosan in biomass combustion aerosol by high-performance anion-exchange chromatography with pulsed amperometric detection, Atmos. Environ., 40, 299–311, doi:10.1016/j.atmosenv.2005.12.069, 2006.

Engling, G., Lee, J. J., Tsai, Y.-W., Lung, S.-C. C., Chou, C. C.-K., and Chan, C.-Y.: Size-resolved anhydrosugar composition in smoke aerosol from controlled field burning of rice straw, Aerosol Sci. Tech., 43, 662–672, doi:10.1080/02786820902825113, 2009.

Feng, Y., Chen, Y., Guo, H., Zhi, G., Xiong, S., Li, J., Sheng, G., and Fu, J.: Characteristics of organic and elemental carbon in $PM_{2.5}$ samples in Shanghai, China, Atmos. Res., 92, 434–442, doi:10.1016/j.atmosres.2009.01.003, 2009.

Fountoukis, C. and Nenes, A.: ISORROPIA II: a computationally efficient thermodynamic equilibrium model for K^+–Ca^{2+}–Mg^{2+}–NH_4^+–Na^+–SO_4^{2-}–NO_3^-–Cl^-–H_2O aerosols, Atmos. Chem. Phys., 7, 4639–4659, doi:10.5194/acp-7-4639-2007, 2007.

Gómez, D. R., Giné, M. F., Bellato, A. C. S., and Smichowski, P.: Antimony: a traffic-related element in the atmosphere of Buenos Aires, Argentina, J. Environ. Monit., 7, 1162–1168, doi:10.1039/B508609D, 2005.

Gregg, J. S., Andres, R. J., and Marland, G.: China: emissions pattern of the world leader in CO_2 emissions from fossil fuel consumption and cement production, Geophys. Res. Lett., 35, L08806, doi:10.1029/2007GL032887, 2008.

Gu, J., Bai, Z., Liu, A., Wu, L., Xie, Y., Li, W., Dong, H., and Zhang, X.: Characterization of atmospheric organic carbon and element carbon of $PM_2.5$ and PM_{10} at Tianjin, China, Aerosol Air Qual. Res., 10, 167–176, doi:10.4209/aaqr.2009.12.0080, 2010.

Hans Wedepohl, K.: The composition of the continental crust, Geochim. Cosmochim. Ac., 59, 1217–1232, doi:10.1016/0016-7037(95)00038-2, 1995.

He, K., Yang, F., Ma, Y., Zhang, Q., Yao, X., Chan, C. K., Cadle, S., Chan, T., and Mulawa, P.: The characteristics of $PM_{2.5}$ in Beijing, China, Atmos. Environ., 35, 4959–4970, doi:10.1016/S1352-2310(01)00301-6, 2001.

Title Page

Abstract | Introduction

Conclusions | References

Tables | Figures

|◄ | ►|

◄ | ►

Back | Close

Full Screen / Esc

Printer-friendly Version

Interactive Discussion

Heo, J.-B., Hopke, P. K., and Yi, S.-M.: Source apportionment of PM$_{2.5}$ in Seoul, Korea, Atmos. Chem. Phys., 9, 4957–4971, doi:10.5194/acp-9-4957-2009, 2009.

Hsu, S., Liu, S., Tsai, F., Engling, G., Lin, I., Chou, C., Kao, S., Lung, S., Chan, C., and Lin, S.: High wintertime particulate matter pollution over an offshore island (Kinmen) off southeastern China: an overview, J. Geophys. Res.-Atmos., 115, D17309, doi:10.1029/2009JD013641, 2010.

Hsu, S.-C., Liu, S. C., Kao, S.-J., Jeng, W.-L., Huang, Y.-T., Tseng, C.-M., Tsai, F., Tu, J.-Y., and Yang, Y.: Water-soluble species in the marine aerosol from the northern South China Sea: high chloride depletion related to air pollution, J. Geophys. Res., 112, D19304, doi:10.1029/2007JD008844, 2007.

Hsu, S.-C., Liu, S. C., Huang, Y.-T., Lung, S.-C. C., Tsai, F., Tu, J.-Y., and Kao, S.-J.: A criterion for identifying Asian dust events based on Al concentration data collected from northern Taiwan between 2002 and early 2007, J. Geophys. Res., 113, D18306, doi:10.1029/2007JD009574, 2008.

Hsu, S. C., Liu, S. C., Huang, Y. T., Chou, C. C. K., Lung, S. C. C., Liu, T. H., Tu, J. Y., and Tsai, F.: Long-range southeastward transport of Asian biosmoke pollution: signature detected by aerosol potassium in Northern Taiwan, J. Geophys. Res., 114, D14301, doi:10.1029/2009JD011725, 2009.

Hsu, S. C., Tsai, F., Lin, F. J., Chen, W. N., Shiah, F. K., Huang Jr, C., Chan, C. Y., Chen, C. C., Liu, T. H., and Chen, H. Y.: A super Asian dust storm over the East and South China Seas: disproportionate dust deposition, J. Geophys. Res.-Atmos., 118, 7169–7181, doi:10.1002/jgrd.50405, 2013.

Hueglin, C., Gehrig, R., Baltensperger, U., Gysel, M., Monn, C., and Vonmont, H.: Chemical characterisation of PM$_{2.5}$, PM$_{10}$ and coarse particles at urban, near-city and rural sites in Switzerland, Atmos. Environ., 39, 637–651, 2005.

Iinuma, Y., Engling, G., Puxbaum, H., and Herrmann, H.: A highly resolved anion-exchange chromatographic method for determination of saccharidic tracers for biomass combustion and primary bio-particles in atmospheric aerosol, Atmos. Environ., 43, 1367–1371, doi:10.1016/j.atmosenv.2008.11.020, 2009.

Khan, M. F., Shirasuna, Y., Hirano, K., and Masunaga, S.: Characterization of PM$_{2.5}$, PM$_{2.5–10}$ and PM$_{10}$ in ambient air, Yokohama, Japan. Atmos. Res., 96, 159–172, doi:10.1016/j.atmosres.2009.12.009, 2010.

Title Page

Abstract | Introduction

Conclusions | References

Tables | Figures

◀◀ | ▶▶

◀ | ▶

Back | Close

Full Screen / Esc

Printer-friendly Version

Interactive Discussion

Laden, F., Neas, L. M., Dockery, D. W., and Schwartz, J.: Association of fine particulate matter from different sources with daily mortality in six US cities, Environ. Health Perspect., 108, 941–947, 2000.

Lee, H. S. and Kang, B.-W.: Chemical characteristics of principal $PM_{2.5}$ species in Chongju, South Korea, Atmos. Environ., 35, 739–746, doi:10.1016/S1352-2310(00)00267-3, 2001.

Lei, Y., Zhang, Q., He, K. B., and Streets, D. G.: Primary anthropogenic aerosol emission trends for China, 1990–2005, Atmos. Chem. Phys., 11, 931–954, doi:10.5194/acp-11-931-2011, 2011.

Lonati, G., Giugliano, M., Butelli, P., Romele, L., and Tardivo, R.: Major chemical components of $PM_{2.5}$ in Milan (Italy), Atmos. Environ., 39, 1925–1934, doi:10.1016/j.atmosenv.2004.12.012, 2005.

Louie, P. K., Watson, J. G., Chow, J. C., Chen, A., Sin, D. W., and Lau, A. K.: Seasonal characteristics and regional transport of $PM_{2.5}$ in Hong Kong, Atmos. Environ., 39, 1695–1710, doi:10.1016/j.atmosenv.2004.11.017, 2005.

Ma, Y., Chen, R., Pan, G., Xu, X., Song, W., Chen, B., and Kan, H.: Fine particulate air pollution and daily mortality in Shenyang, China, Sci. Total Environ. 409, 2473–2477, doi:10.1016/j.scitotenv.2011.03.017, 2011.

Machemer, S. D.: Characterization of airborne and bulk particulate from iron and steel manufacturing facilities, Environ. Sci. Technol., 38, 381–389, doi:10.1021/es020897v, 2004.

Malm, W. C., Sisler, J. F., Huffman, D., Eldred, R. A., and Cahill, T. A.: Spatial and seasonal trends in particle concentration and optical extinction in the United States, J. Geophys. Res., 99, 1347–1370, doi:10.1029/93JD02916, 1994.

Mamane, Y., Perrino, C., Yossef, O., and Catrambone, M.: Source characterization of fine and coarse particles at the East Mediterranean coast, Atmos. Environ. 42, 6114–6130, doi:10.1016/j.atmosenv.2008.02.045, 2008.

Mooibroek, D., Schaap, M., Weijers, E., and Hoogerbrugge, R.: Source apportionment and spatial variability of $PM_{2.5}$ using measurements at five sites in the Netherlands, Atmos. Environ., 45, 4180–4191, doi:10.1016/j.atmosenv.2011.05.017, 2011.

Mukai, H., Tanaka, A., Fujii, T., Zeng, Y., Hong, Y., Tang, J., Guo, S., Xue, H., Sun, Z., and Zhou, J.: Regional characteristics of sulfur and lead isotope ratios in the atmosphere at several Chinese urban sites, Environ. Sci. Technol., 35, 1064–1071, doi:10.1021/es001399u, 2001.

Negral, L., Moreno-Grau, S., Moreno, J., Querol, X., Viana, M., and Alastuey, A.: Natural and anthropogenic contributions to PM$_{10}$ and PM$_{2.5}$ in an urban area in the western Mediterranean coast, Water Air Soil Pollut., 192, 227–238, doi:10.1007/s11270-008-9650-y, 2008.

Ni, Z.-Y., Chen, Y.-J., Li, N., and Zhang, H.: Pb–Sr–Nd isotope constraints on the fluid source of the Dahu Au–Mo deposit in Qinling Orogen, central China, and implication for Triassic tectonic setting, Ore Geol. Rev., 46, 60–67, doi:10.1016/j.oregeorev.2012.01.004, 2012.

Norris, G., Vedantham, R., Wade, K., Brown, S., Prouty, J., and Foley, C.: EPA positive matrix factorization (PMF) 3.0 fundamentals & user guide, US Environmental Protection Agency, Office of Research and Development, Washington DC, 2008.

Oliveira, C., Pio, C., Alves, C., Evtyugina, M., Santos, P., Gonçalves, V., Nunes, T., Silvestre, A. J., Palmgren, F., and Wåhlin, P.: Seasonal distribution of polar organic compounds in the urban atmosphere of two large cities from the North and South of Europe, Atmos. Environ., 41, 5555–5570, doi:10.1016/j.atmosenv.2007.03.001, 2007.

Pacyna, J. M. and Pacyna, E. G.: An assessment of global and regional emissions of trace metals to the atmosphere from anthropogenic sources worldwide, Environ. Rev., 9, 269–298, doi:10.1139/a01-012, 2001.

Pekney, N. J., Davidson, C. I., Robinson, A., Zhou, L., Hopke, P., Eatough, D., and Rogge, W. F.: Major source categories for PM$_{2.5}$ in Pittsburgh using PMF and UNMIX, Aerosol Sci. Tech., 40, 910–924, doi:10.1080/02786820500380271, 2006.

Pinto, J. P., Lefohn, A. S., and Shadwick, D. S.: Spatial Variability of PM$_{2.5}$ in Urban Areas in the United States, J. Air Waste Manage. Assoc., 54, 440–449, doi:10.1080/10473289.2004.10470919, 2004.

Pio, C., Legrand, M., Alves, C., Oliveira, T., Afonso, J., Caseiro, A., Puxbaum, H., Sánchez-Ochoa, A., and Gelencsér, A.: Chemical composition of atmospheric aerosols during the 2003 summer intense forest fire period, Atmos. Environ., 42, 7530–7543, doi:10.1016/j.atmosenv.2008.05.032, 2008.

Pope III, C. A. and Dockery, D. W.: Health effects of fine particulate air pollution: lines that connect, J. Air Waste Manage. Assoc., 56, 709–742, doi:10.1080/10473289.2006.10464485, 2006.

Putaud, J.-P., Raes, F., Van Dingenen, R., Brüggemann, E., Facchini, M., Decesari, S., Fuzzi, S., Gehrig, R., Hüglin, C., and Laj, P.: A European aerosol phenomenology – 2: chemical characteristics of particulate matter at kerbside, urban, rural and background sites in Europe, Atmos. Environ., 38, 2579–2595, doi:10.1016/j.atmosenv.2004.01.041, 2004.

Title Page

Abstract | Introduction

Conclusions | References

Tables | Figures

◀ | ▶

◀ | ▶

Back | Close

Full Screen / Esc

Printer-friendly Version

Interactive Discussion

Qin, Y. and Xie, S. D.: Spatial and temporal variation of anthropogenic black carbon emissions in China for the period 1980–2009, Atmos. Chem. Phys., 12, 4825–4841, doi:10.5194/acp-12-4825-2012, 2012.

Querol, X., Alastuey, A., Ruiz, C., Artinano, B., Hansson, H., Harrison, R., Buringh, E. T., Ten Brink, H., Lutz, M., and Bruckmann, P.: Speciation and origin of PM_{10} and $PM_{2.5}$ in selected European cities, Atmos. Environ., 38, 6547–6555, doi:10.1016/j.atmosenv.2004.08.037, 2004.

Querol, X., Zhuang, X., Alastuey, A., Viana, M., Lv, W., Wang, Y., López, A., Zhu, Z., Wei, H., and Xu, S.: Speciation and sources of atmospheric aerosols in a highly industrialised emerging mega-city in Central China, J. Environ. Monit., 8, 1049–1059, doi:10.1039/B608768J, 2006.

Sheesley, R. J., Schauer, J. J., Chowdhury, Z., Cass, G. R., and Simoneit, B. R.: Characterization of organic aerosols emitted from the combustion of biomass indigenous to South Asia, J. Geophys. Res., 108, 4285, doi:10.1029/2002JD002981, 2003.

Simon, H., Bhave, P. V., Swall, J. L., Frank, N. H., and Malm, W. C.: Determining the spatial and seasonal variability in OM/OC ratios across the US using multiple regression, Atmos. Chem. Phys., 11, 2933–2949, doi:10.5194/acp-11-2933-2011, 2011.

Sternbeck, J., Sjödin, Å., and Andréasson, K.: Metal emissions from road traffic and the influence of resuspension – results from two tunnel studies, Atmos. Environ. 36, 4735–4744, doi:10.1016/S1352-2310(02)00561-7, 2002.

Sweet, C. W., Vermette, S. J., and Landsberger, S.: Sources of toxic trace elements in urban air in Illinois, Environ. Sci. Technol., 27, 2502–2510, doi:10.1021/es00048a030, 1993.

Szidat, S., Jenk, T. M., Synal, H. A., Kalberer, M., Wacker, L., Hajdas, I., Kasper-Giebl, A., and Baltensperger, U.: Contributions of fossil fuel, biomass burning, and biogenic emissions to carbonaceous aerosols in Zurich as traced by ^{14}C, J. Geophys. Res.-Atmos., 111, D07206, doi:10.1029/2005JD006590, 2006.

Szidat, S., Ruff, M., Perron, N., Wacker, L., Synal, H.-A., Hallquist, M., Shannigrahi, A. S., Yttri, K. E., Dye, C., and Simpson, D.: Fossil and non-fossil sources of organic carbon (OC) and elemental carbon (EC) in Göteborg, Sweden, Atmos. Chem. Phys., 9, 1521–1535, doi:10.5194/acp-9-1521-2009, 2009.

Tao, J., Shen, Z., Zhu, C., Yue, J., Cao, J., Liu, S., Zhu, L., and Zhang, R.: Seasonal variations and chemical characteristics of sub-micrometer particles (PM_1) in Guangzhou, China, Atmos. Res., 115, 222–231, doi:10.1016/j.atmosres.2012.06.025, 2012.

Title Page

Abstract | Introduction

Conclusions | References

Tables | Figures

◄ | ►

◄ | ►

Back | Close

Full Screen / Esc

Printer-friendly Version

Interactive Discussion

Tao, J., Zhang, L., Engling, G., Zhang, R., Yang, Y., Cao, J., Zhu, C., Wang, Q., and Luo, L.: Chemical composition of $PM_{2.5}$ in an urban environment in Chengdu, China: importance of springtime dust storms and biomass burning, Atmos. Res., 122, 270–283, doi:10.1016/j.atmosres.2012.11.004, 2013.

Tao, J., Zhang, L., Ho, K., Zhang, R., Lin, Z., Zhang, Z., Lin, M., Cao, J., Liu, S., and Wang, G.: Impact of $PM_{2.5}$ chemical compositions on aerosol light scattering in Guangzhou – the largest megacity in South China, Atmos. Res., 135–136, 48–58, doi:10.1016/j.atmosres.2013.08.015, 2014.

Taylor, S. R.: Trace element abundances and the chondritic Earth model, Geochim. Cosmochim. Ac., 28, 1989–1998, doi:10.1016/0016-7037(64)90142-5, 1964.

Tian, H. Z., Wang, Y., Xue, Z. G., Cheng, K., Qu, Y. P., Chai, F. H., and Hao, J. M.: Trend and characteristics of atmospheric emissions of Hg, As, and Se from coal combustion in China, 1980–2007, Atmos. Chem. Phys., 10, 11905–11919, doi:10.5194/acp-10-11905-2010, 2010.

Tian, H., Zhao, D., Cheng, K., Lu, L., He, M., and Hao, J.: Anthropogenic atmospheric emissions of antimony and its spatial distribution characteristics in China, Environ. Sci. Technol., 46, 3973–3980, doi:10.1021/es2041465, 2012.

Tsukuda, S., Sugiyama, M., Harita, Y., and Nishimura, K.: Atmospheric bulk deposition of soluble phosphorus in Ashiu Experimental Forest, Central Japan: source apportionment and sample contamination problem, Atmos. Environ. 39, 823–836, doi:10.1016/j.atmosenv.2004.10.028, 2005.

Turpin, B. J. and Huntzicker, J. J.: Identification of secondary organic aerosol episodes and quantitation of primary and secondary organic aerosol concentrations during SCAQS, Atmos. Environ., 29, 3527–3544, doi:10.1016/1352-2310(94)00276-Q, 1995.

Turpin, B. J. and Lim, H.-J.: Species contributions to $PM_{2.5}$ mass concentrations: revisiting common assumptions for estimating organic mass, Aerosol Sci. Tech., 35, 602–610, doi:10.1080/02786820119445, 2001.

Varrica, D., Bardelli, F., Dongarrà, G., and Tamburo, E.: Speciation of Sb in airborne particulate matter, vehicle brake linings, and brake pad wear residues. Atmos. Environ., 64, doi:10.1016/j.atmosenv.2012.08.067, 18–24.

Wang, X., Zhang, L., and Moran, M. D.: Uncertainty assessment of current size-resolved parameterizations for below-cloud particle scavenging by rain, Atmos. Chem. Phys., 10, 5685–5705, doi:10.5194/acp-10-5685-2010, 2010.

Title Page

Abstract | Introduction

Conclusions | References

Tables | Figures

◄ | ►

◄ | ►

Back | Close

Full Screen / Esc

Printer-friendly Version

Interactive Discussion

Watson, J. G.: Visibility: science and regulation, JAPCA J. Air Waste Ma., 52, 628–713, doi:10.1080/10473289.2002.10470813, 2002.

Watson, J. G., Chow, J. C., and Houck, J. E.: $PM_{2.5}$ chemical source profiles for vehicle exhaust, vegetative burning, geological material, and coal burning in Northwestern Colorado during 1995, Chemosphere, 43, 1141–1151, doi:10.1016/S0045-6535(00)00171-5, 2001.

Xing, L., Fu, T.-M., Cao, J. J., Lee, S. C., Wang, G. H., Ho, K. F., Cheng, M.-C., You, C.-F., and Wang, T. J.: Seasonal and spatial variability of the OM/OC mass ratios and high regional correlation between oxalic acid and zinc in Chinese urban organic aerosols, Atmos. Chem. Phys., 13, 4307–4318, doi:10.5194/acp-13-4307-2013, 2013.

Xu, H., Cao, J., Ho, K., Ding, H., Han, Y., Wang, G., Chow, J., Watson, J., Khol, S., and Qiang, J.: Lead concentrations in fine particulate matter after the phasing out of leaded gasoline in Xi'an, China, Atmos. Environ., 46, 217–224, doi:10.1016/j.atmosenv.2011.09.078, 2012a.

Xu, L., Chen, X., Chen, J., Zhang, F., He, C., Zhao, J., and Yin, L.: Seasonal variations and chemical compositions of $PM_{2.5}$ aerosol in the urban area of Fuzhou, China, Atmos. Res., 104, 264–272, doi:10.1016/j.atmosres.2011.10.017, 2012b.

Yang, F., Tan, J., Zhao, Q., Du, Z., He, K., Ma, Y., Duan, F., Chen, G., and Zhao, Q.: Characteristics of $PM_{2.5}$ speciation in representative megacities and across China, Atmos. Chem. Phys., 11, 5207–5219, doi:10.5194/acp-11-5207-2011, 2011.

Yang, H.-H., Lai, S.-O., Hsieh, L.-T., Hsueh, H.-J., and Chi, T.-W.: Profiles of PAH emission from steel and iron industries, Chemosphere, 48, 1061–1074, doi:10.1016/S0045-6535(02)00175-3, 2002.

Ye, B., Ji, X., Yang, H., Yao, X., Chan, C. K., Cadle, S. H., Chan, T., and Mulawa, P. A.: Concentration and chemical composition of $PM_{2.5}$ in Shanghai for a 1-year period, Atmos. Environ., 37, 499–510, doi:10.1016/S1352-2310(02)00918-4, 2003.

Yttri, K. E., Dye, C., Braathen, O.-A., Simpson, D., and Steinnes, E.: Carbonaceous aerosols in Norwegian urban areas, Atmos. Chem. Phys., 9, 2007–2020, doi:10.5194/acp-9-2007-2009, 2009.

Zdráhal, Z., Oliveira, J., Vermeylen, R., Claeys, M., and Maenhaut, W.: Improved method for quantifying levoglucosan and related monosaccharide anhydrides in atmospheric aerosols and application to samples from urban and tropical locations, Environ. Sci. Technol., 36, 747–753, doi:10.1021/es015619v, 2002.

Zhang, F., Xu, L., Chen, J., Yu, Y., Niu, Z., and Yin, L.: Chemical compositions and extinction coefficients of $PM_{2.5}$ in peri-urban of Xiamen, China, during June 2009–May 2010, Atmos. Res., 106, 150–158, doi:10.1016/j.atmosres.2011.12.005, 2012.

Zhang, R., Jing, J., Tao, J., Hsu, S.-C., Wang, G., Cao, J., Lee, C. S. L., Zhu, L., Chen, Z., Zhao, Y., and Shen, Z.: Chemical characterization and source apportionment of $PM_{2.5}$ in Beijing: seasonal perspective, Atmos. Chem. Phys., 13, 7053–7074, doi:10.5194/acp-13-7053-2013, 2013.

Zhang, T., Cao, J., Tie, X., Shen, Z., Liu, S., Ding, H., Han, Y., Wang, G., Ho, K., and Qiang, J.: Water-soluble ions in atmospheric aerosols measured in Xi'an, China: seasonal variations and sources, Atmos. Res., 102, 110–119, doi:10.1016/j.atmosres.2011.06.014, 2011.

Zhang, X. Y., Wang, Y. Q., Zhang, X. C., Guo, W., and Gong, S. L.: Carbonaceous aerosol composition over various regions of China during 2006, J. Geophys. Res., 113, D14111, doi:10.1029/2007JD009525, 2008a.

Zhang, Y., Schauer, J. J., Zhang, Y., Zeng, L., Wei, Y., Liu, Y., and Shao, M.: Characteristics of particulate carbon emissions from real-world Chinese coal combustion, Environ. Sci. Technol., 42, 5068–5073, doi:10.1021/es7022576, 2008b.

Zhao, Q., He, K., Rahn, K. A., Ma, Y., Jia, Y., Yang, F., Duan, F., Lei, Y., G, Chen, Cheng, Y., H, Liu, and Wang, S.: Dust storms come to Central and Southwestern China, too: implications from a major dust event in Chongqing, Atmos. Chem. Phys., 10, 2615–2630, doi:10.5194/acp-10-2615-2010, 2010.

Title Page

Abstract | Introduction

Conclusions | References

Tables | Figures

|◄ | ►|

◄ | ►

Back | Close

Full Screen / Esc

Printer-friendly Version

Interactive Discussion

Table 1. Statistics of annual PM$_{2.5}$ mass concentrations in urban Chengdu and other cities in the world.

City/Nation	Sampling period	PM$_{2.5}$ ($\mu g\,m^{-3}$)	Reference
Chengdu, Southwest China	2011	119	This study
Chongqing, Southwest China	2005–2006	129.0	Yang et al. (2011)
Xi'an, Northwest China	2009	194.1	Zhang et al. (2011)
Beijing, North China	2009–2010	135.0	Zhang et al. (2013)
Tianjin, North China	2008	109.8	Gu et al. (2010)
Shenyang, Northeast China	2006–2008	75	Ma et al. (2011)
Shanghai, East China	2005–2006	90.3	Feng et al. (2009)
Fuzhou, Southeast China	2007–2008	44.33	Xu et al. (2012)
Xiamen, Southeast China	2009–2010	86.16	Zhang et al. (2012)
Guangzhou, South China	2009–2010	76.0	Tao et al. (2014)
Hong Kong, South China	2000–2001	56.7	Louie et al. (2005)
Seoul, Korea	2003–2006	43.5	Heo et al. (2009)
Yokohama, Japan	2007–2008	20.6	Khan et al. (2009)
Singapore, Singapore	2000	27.2	Balasubramanian et al. (2003)
27 urban sites, US	1999–2000	< 35	Pinto et al. (2004)
Austria, Germany, Switzerland, the Netherlands, UK (central EU)	1998–2002	16–30	Querol et al. (2004)
Sweden (Northern EU)	1998–2002	8–15	Querol et al. (2004)
Spain (Southern EU)	1998–2002	19–25	Querol et al. (2004)

Table 2. Statistics of PM$_{2.5}$ chemical components in four seasons.

	Annual (*n* = 117)	Spring (*n* = 31)	Summer (*n* = 30)	Autumn (*n* = 31)	Winter (*n* = 25)
PM$_{2.5}$/µg m^{-3}	119 ± 56	126 ± 66	89 ± 35	111 ± 49	158 ± 51
OC/µg m^{-3}	17 ± 8	15 ± 7	11 ± 4	20 ± 9	22 ± 7
EC/µg m^{-3}	7 ± 4	7 ± 5	6 ± 3	7 ± 3	8 ± 4
Na$^+$/µg m^{-3}	0.6 ± 0.3	0.7 ± 0.3	0.5 ± 0.2	0.5 ± 0.3	0.5 ± 0.2
NH$_4^+$/µg m^{-3}	11.6 ± 7.3	11.9 ± 10.0	9.0 ± 5.0	11.1 ± 6.0	15.3 ± 5.7
K$^+$/µg m^{-3}	1.7 ± 0.8	1.5 ± 0.8	1.3 ± 0.6	1.8 ± 0.7	2.1 ± 0.7
Mg^{2+}/µg m^{-3}	0.1 ± 0.0	0.1 ± 0.1	0.1 ± 0.0	0.0 ± 0.0	0.1 ± 0.0
Ca^{2+}/µg m^{-3}	0.4 ± 0.3	0.6 ± 0.4	0.3 ± 0.2	0.3 ± 0.1	0.3 ± 0.1
F$^-$/µg m^{-3}	0.1 ± 0.1	0.1 ± 0.1	0.0 ± 0.0	0.1 ± 0.1	0.1 ± 0.0
Cl$^-$/µg m^{-3}	1.7 ± 1.7	1.5 ± 1.5	0.4 ± 0.4	2.5 ± 1.6	2.8 ± 1.9
NO$_3^-$/µg m^{-3}	10.7 ± 7.8	10.2 ± 8.7	5.3 ± 3.2	12.9 ± 8.5	15.5 ± 5.4
SO$_4^{2-}$/µg m^{-3}	25.0 ± 14.1	26.4 ± 18.1	23.7 ± 13.5	19.2 ± 9.6	31.8 ± 10.7
LG/ng m^{-3}	412 ± 352	235 ± 151	152 ± 89	659 ± 441	635 ± 246
MN/ng m^{-3}	34 ± 35	19 ± 17	9 ± 7	36 ± 27	80 ± 34
Al/ng m^{-3}	560 ± 420	898 ± 581	427 ± 331	462 ± 217	426 ± 201
Fe/ng m^{-3}	693 ± 420	899 ± 561	610 ± 363	640 ± 303	606 ± 335
Na/ng m^{-3}	837 ± 680	865 ± 413	736 ± 342	847 ± 344	658 ± 283
Mg/ng m^{-3}	196 ± 164	299 ± 251	147 ± 123	166 ± 78	164 ± 86
K/ng m^{-3}	1576 ± 751	1575 ± 876	1312 ± 623	1757 ± 777	1681 ± 640
Ca/ng m^{-3}	402 ± 339	588 ± 440	341 ± 344	389 ± 218	262 ± 203
Sr/ng m^{-3}	5.7 ± 4.1	7.5 ± 4.9	3.6 ± 2.5	5.4 ± 3.1	6.6 ± 4.6
Ba/ng m^{-3}	22 ± 17	26 ± 13	13 ± 6	23 ± 15	30 ± 24
Ti/ng m^{-3}	50 ± 33	71 ± 43	46 ± 32	47 ± 23	35 ± 17
Mn/ng m^{-3}	66 ± 37	78 ± 51	59 ± 28	63 ± 32	65 ± 28
Ni/ng m^{-3}	2.5 ± 1.6	2.5 ± 1.4	2.0 ± 0.8	2.6 ± 1.5	3.2 ± 2.3
Cu/ng m^{-3}	23 ± 12	26 ± 15	23 ± 10	18 ± 10	27 ± 12
Zn/ng m^{-3}	350 ± 230	440 ± 318	324 ± 182	310 ± 164	319 ± 205
Mo/ng m^{-3}	3.8 ± 3.8	2.6 ± 1.7	2.7 ± 1.5	4.6 ± 4.3	5.4 ± 5.8
Cd/ng m^{-3}	3.5 ± 1.9	4.1 ± 2.4	3.1 ± 1.5	3.0 ± 1.6	4.0 ± 2.0
Sn/ng m^{-3}	10.6 ± 6.9	12.7 ± 9.3	9.0 ± 4.7	9.7 ± 5.9	11.0 ± 6.6
Sb/ng m^{-3}	6.5 ± 4.2	8.2 ± 5.5	4.8 ± 2.4	5.2 ± 2.9	8.1 ± 4.3
Tl/ng m^{-3}	1.9 ± 1.1	2.5 ± 1.6	1.4 ± 0.4	1.6 ± 0.8	2.3 ± 1.1
Pb/ng m^{-3}	172 ± 86	198 ± 107	142 ± 58	154 ± 68	198 ± 94
V/ng m^{-3}	1.7 ± 0.9	2.2 ± 1.2	1.4 ± 0.7	1.6 ± 0.7	1.6 ± 0.6
Cr/ng m^{-3}	9.2 ± 5.0	10.0 ± 6.4	9.7 ± 3.8	8.6 ± 5.0	8.3 ± 4.2
As/ng m^{-3}	20 ± 11	19 ± 12	21 ± 12	22 ± 10	18 ± 10
Se/ng m^{-3}	2.7 ± 1.2	2.9 ± 1.6	2.3 ± 0.7	2.9 ± 1.3	2.9 ± 1.0
Zr/ng m^{-3}	2.8 ± 1.6	4.0 ± 1.9	2.3 ± 1.2	2.5 ± 1.3	2.4 ± 1.2
Ge/ng m^{-3}	1.1 ± 0.6	1.2 ± 0.7	0.9 ± 0.3	1.0 ± 0.5	1.2 ± 0.5
Rb/ng m^{-3}	7.6 ± 3.7	8.6 ± 5.0	6.6 ± 2.7	7.2 ± 3.2	8.2 ± 3.0
Cs/ng m^{-3}	1.2 ± 0.6	1.1 ± 0.7	1.2 ± 0.6	1.3 ± 0.7	1.2 ± 0.5
Ga/ng m^{-3}	5.8 ± 3.1	5.9 ± 3.5	5.1 ± 2.1	6.3 ± 3.5	5.8 ± 3.1
Si[a]/ng m^{-3}	1204 ± 860	1962 ± 1142	933 ± 719	868 ± 392	1020 ± 351

[a]: Si analysis by XRF method.

Table 3. The calculated chemical components and phase state of ions (μg m^{-3}) in lab condition (Temp = 23°, RH = 40 %) in Chengdu. Results were modeled by the ISORROPIA II.

	Annual (n = 117)	Spring (n = 31)	Summer (n = 30)	Autumn (n = 31)	Winter (n = 25)
$(NH_4)_2SO_4$	28.3 ± 18.1	29.2 ± 23.1	27.5 ± 17.6	20.7 ± 12.0	37.4 ± 13.8
Na_2SO_4	1.8 ± 0.9	2.2 ± 1.0	1.6 ± 0.7	1.7 ± 0.8	1.6 ± 0.7
K_2SO_4	3.8 ± 1.7	3.4 ± 1.9	3.0 ± 1.3	4.1 ± 1.7	4.7 ± 1.6
$MgSO_4$	0.3 ± 0.2	0.5 ± 0.4	0.3 ± 0.2	0.2 ± 0.1	0.4 ± 0.2
$CaSO_4$	1.2 ± 0.9	2.0 ± 1.3	0.9 ± 0.7	0.9 ± 0.5	1.0 ± 0.4
NH_4NO_3	13.5 ± 10.3	12.8 ± 11.3	5.9 ± 4.3	16.7 ± 10.9	19.6 ± 7.3
NH_4Cl	1.9 ± 2.5	1.6 ± 2.4	0.3 ± 0.4	3.7 ± 2.3	2.1 ± 2.7
H_2O(aq)	15.0 ± 8.4	15.3 ± 10.6	12.4 ± 6.9	13.1 ± 6.8	19.8 ± 6.9
Σ species	64.2 ± 36.4	66.7 ± 46.9	50.9 ± 27.3	58.2 ± 30.9	84.7 ± 29.3
Σ species/PM$_{2.5}$(%)	54.8 ± 16.1	51.2 ± 14.6	61.7 ± 20.6	51.2 ± 16.0	55.3 ± 6.7

Table 4. The contributions from six identified sources of PM$_{2.5}$ in Chengdu.

Sources	Annual		Spring		Summer		Autumn		Winter	
	µg m^{-3}	%	µg m^{-3}	%	µg m^{-3}	%	µg m^{-3}	%	µg m^{-3}	%
Secondary inorganic aerosols	46 ± 32	37 ± 18	47 ± 37	37 ± 16	35 ± 24	37 ± 20	38 ± 28	33 ± 18	67 ± 29	44 ± 17
Coal combustion	22 ± 18	20 ± 12	29 ± 23	22 ± 12	20 ± 12	23 ± 12	13 ± 14	14 ± 13	29 ± 19	18 ± 9
Biomass burning	15 ± 17	11 ± 10	9 ± 9	7 ± 6	2 ± 4	1 ± 5	24 ± 17	19 ± 11	27 ± 17	16 ± 7
Iron and steel industry	13 ± 11	11 ± 9	12 ± 13	8 ± 7	16 ± 8	19 ± 9	13 ± 11	11 ± 8	8 ± 7	5 ± 4
Mo-related industry	12 ± 10	11 ± 9	8 ± 5	8 ± 5	7 ± 6	11 ± 14	15 ± 10	14 ± 7	20 ± 10	13 ± 5
Soil dust	10 ± 10	10 ± 12	18 ± 14	18 ± 17	8 ± 9	9 ± 12	8 ± 5	8 ± 7	4 ± 6	4 ± 5
Simulated PM$_{2.5}$ by PMF	118 ± 56	100	123 ± 68	100	88 ± 34	100	110 ± 49	100	155 ± 48	100
Measured PM$_{2.5}$	119 ± 56		126 ± 66		89 ± 35		111 ± 49		158 ± 51	

Table 5. Summary of Measures have been taken by local and national government in Chengdu.

Source	Measures taken by local government	Measures taken by national government
Secondary inorganic aerosols	All industrial factories relocated out Chengdu urban area	Industrial emission standard
Coal combustion	Coal combustion were forbidden in urban area	Industrial emission standard
Biomass burning	Establish special management committee	None
Iron and steel industry	None	Industrial emission standard
Mo-related industry	None	None
Traffic emissions	Hybrid electric vehicles used in public transportation system	Emission standards for new vehicles
Soil dust	None	None
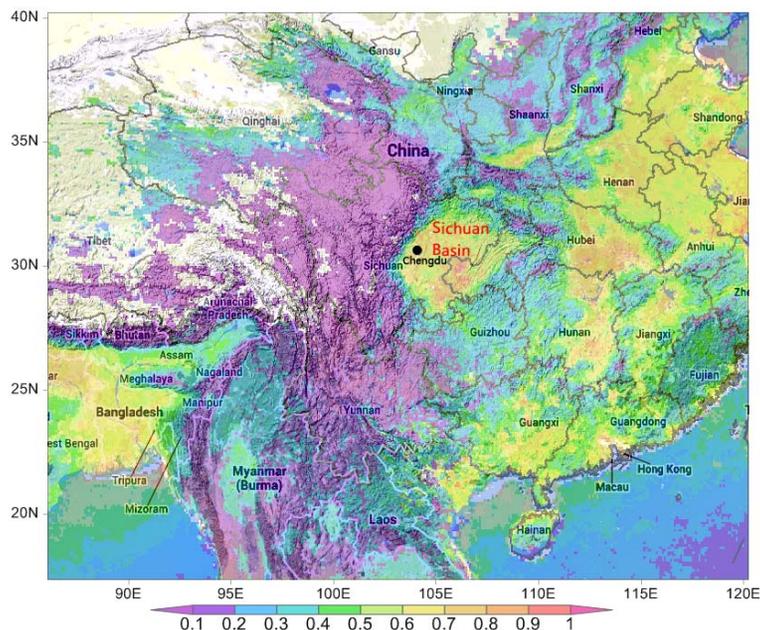
Fig. 1. Sampling location (30.65° N, 104.03° E) in Chengdu on a regional map superimposed with spatial distribution of annual mean aerosol optical depth (AOD) retrieved from MODIS satellite remote sensing in 2011.
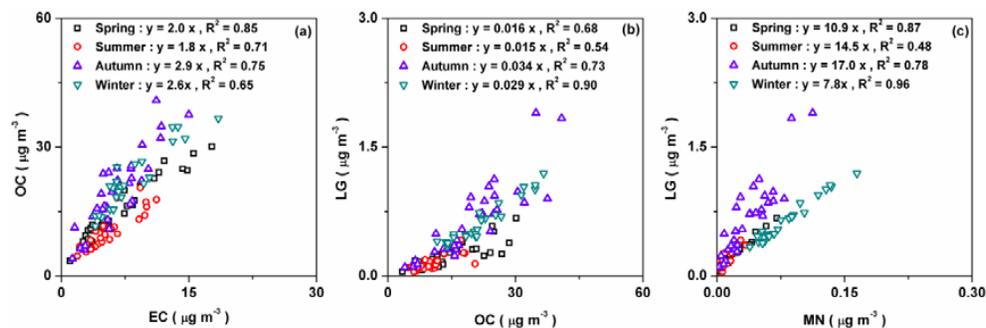
Fig. 2. Scatter plots of OC vs. EC **(a)**, LG vs. OC **(b)** and LG vs. MN **(c)** in four seasons. Also shown are the linear regression lines with regression equations.
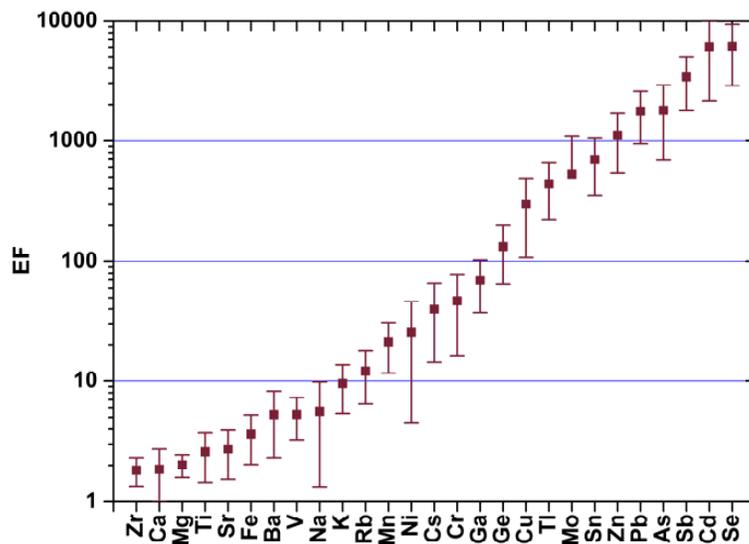
Fig. 3. Enrichment factors of trace elements.

Title Page

Abstract | Introduction

Conclusions | References

Tables | Figures

|◀ | ▶|

◀ | ▶

Back | Close

Full Screen / Esc

Printer-friendly Version

Interactive Discussion
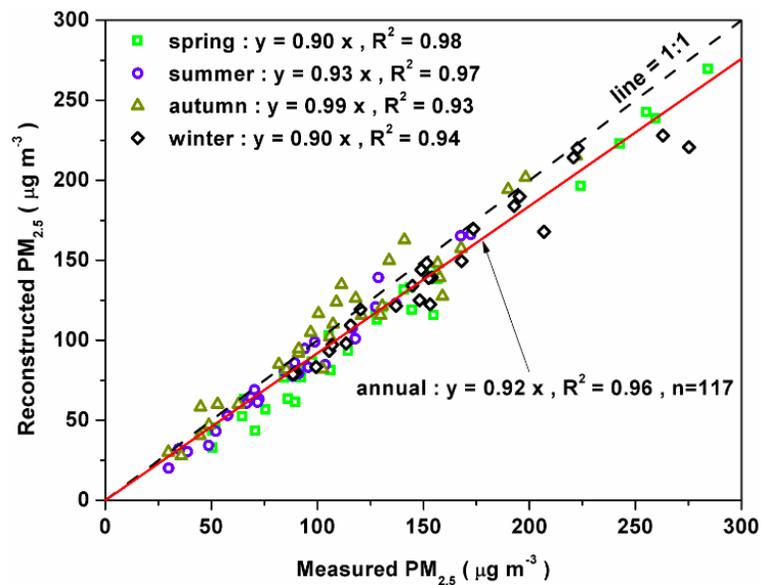
Fig. 4. Correlation between reconstructed and measured PM$_{2.5}$ mass concentrations in four seasons. Also shown are the linear regression lines with regression equations.
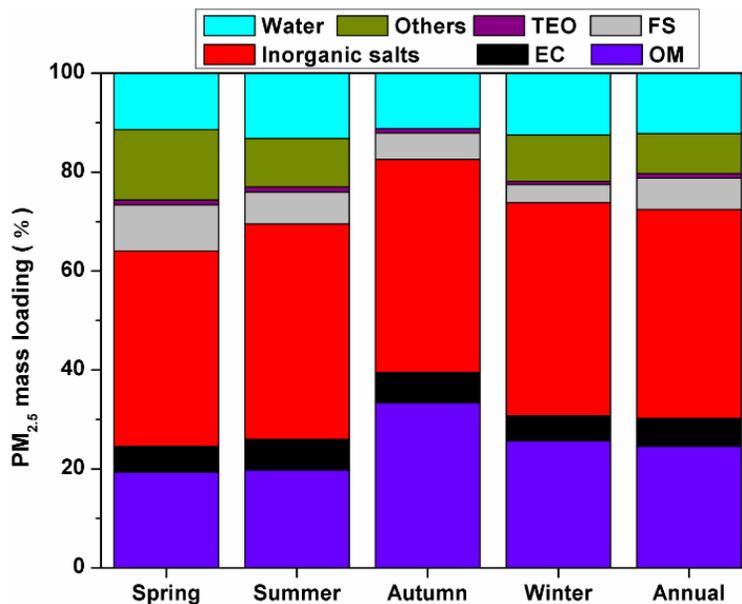
Fig. 5. Chemical mass closures of PM2.5 mass concentrations in four seasons. The major chemical components include inorganic salts, organic matter (OM), elemental carbon (EC), fine soil (FS), trace element oxides (TEO), water content, as well as others that were unidentified.
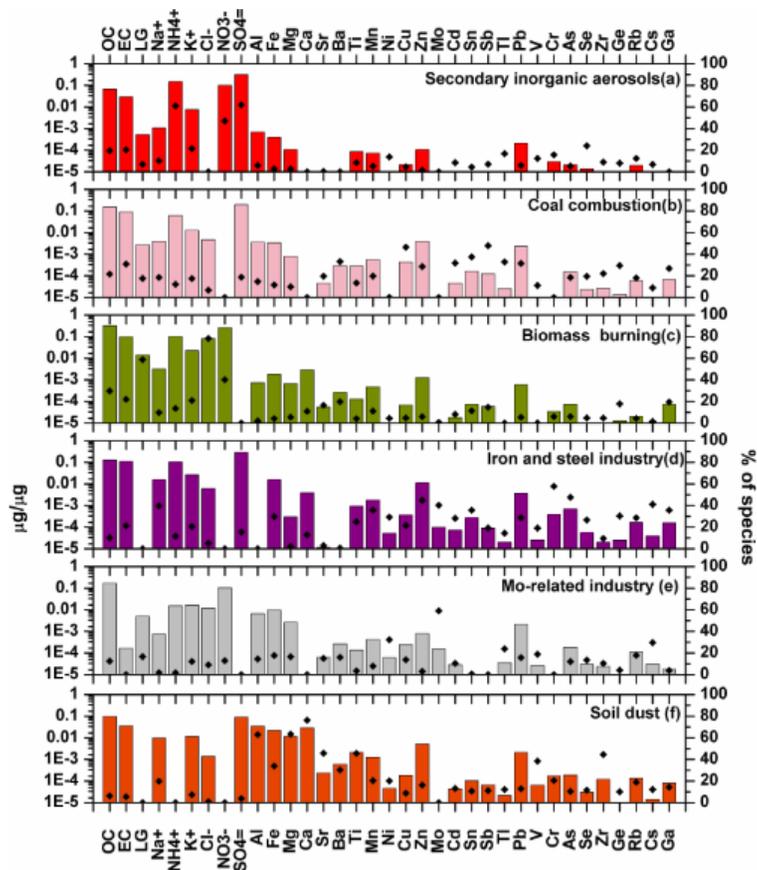
Fig. 6. Six source profiles (bars) resolved from the PMF model (in unit µg µg^{-1}). Also shown is contribution percentages (black dots) from each source factor (in unit %).
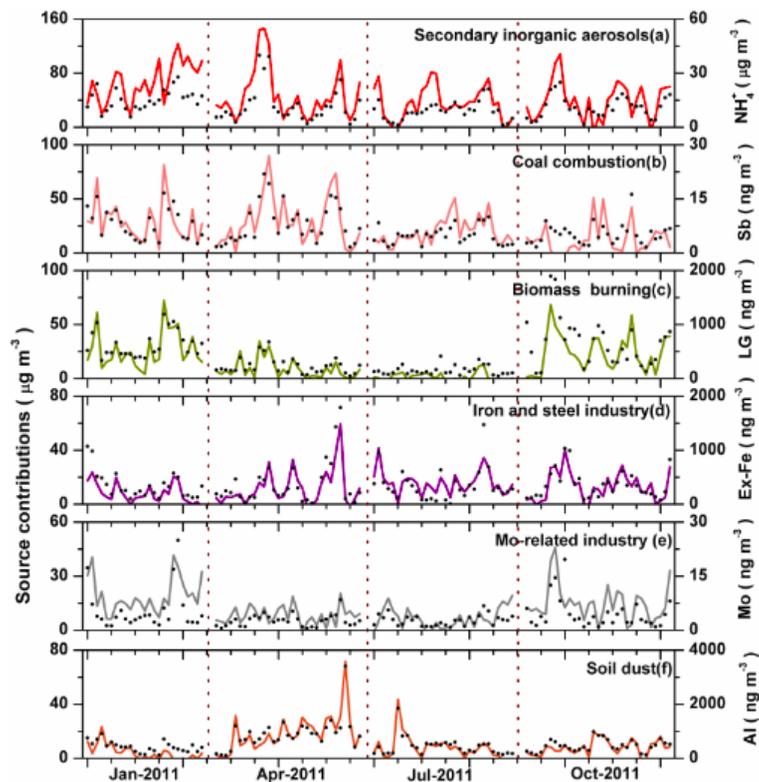
Fig. 7. Time series of daily contributions from each identified source (continuous line) and specific chemical species (black dot) between January and October 2011.

Title Page

Abstract | Introduction

Conclusions | References

Tables | Figures

|◄ | ►|

◄ | ►

Back | Close

Full Screen / Esc

Printer-friendly Version

Interactive Discussion
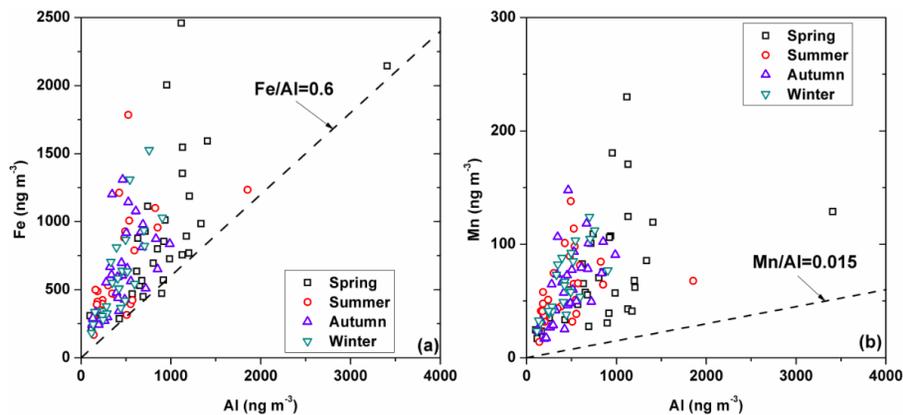
Fig. 8. Scatter plots of Fe vs. Al and Mn vs. Al in PM$_{2.5}$ of Chengdu.
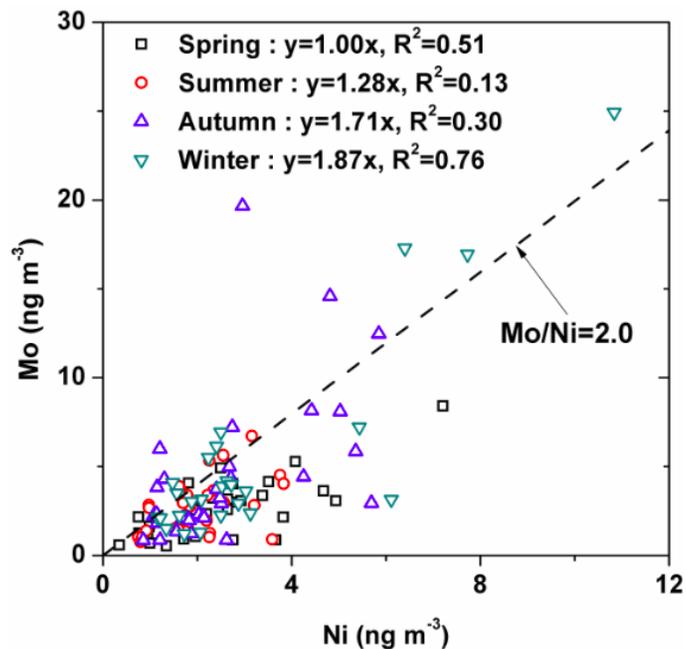
Fig. 9. Scatter plots of Mo and Ni in four seasons.
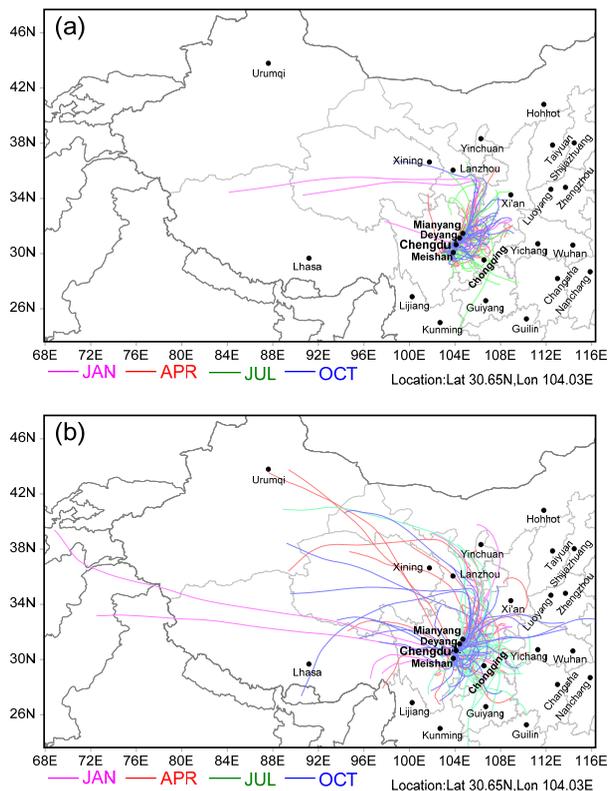
Fig. 10. Analytical results of the 48 h air mass back trajectories at 500 m **(a)** and 1500 m **(b)** elevation during the sampling periods, which were run four times per day.

Title Page

Abstract | Introduction

Conclusions | References

Tables | Figures

|◄ | ►|

◄ | ►

Back | Close

Full Screen / Esc

Printer-friendly Version

Interactive Discussion